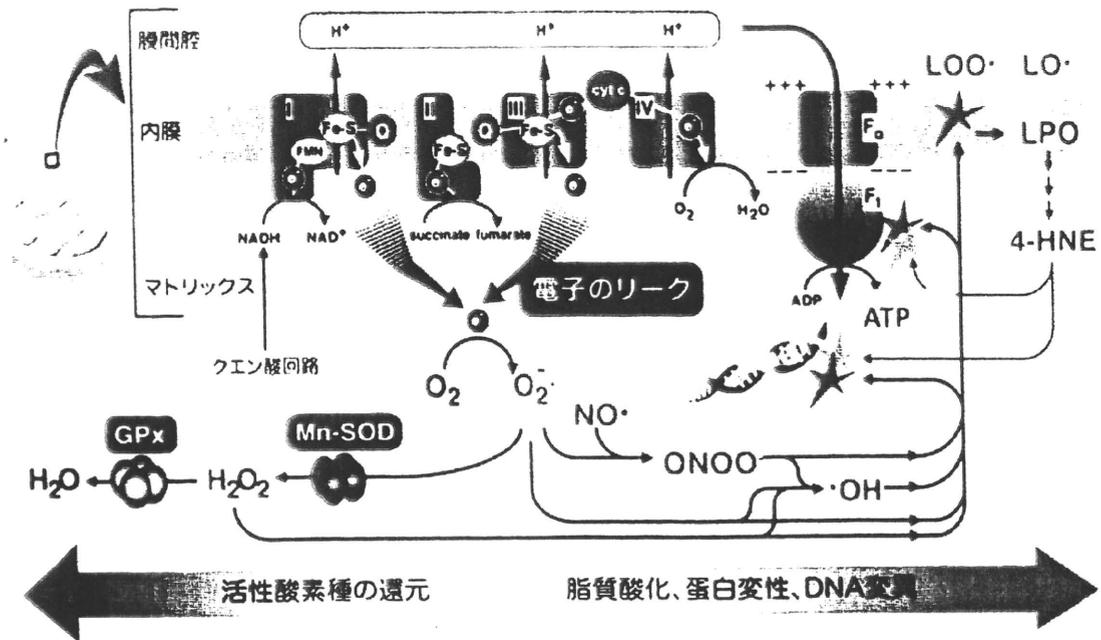# ミトコンドリアは発電所

ミトコンドリアが電気エネルギーをATPのエネルギーに変える



## ミトコンドリアにおける活性酸素種の発生と代謝

図1　ミトコンドリアにおける活性酸素種の生成と消去の概略

　ミトコンドリアの内膜の電子伝達系から遊離した電子（e⁻）は$O_2$に吸収され，$\cdot O_2^-$が生じる。$\cdot O_2^-$は，MnSODによって$H_2O_2$に変換され，GPx（グルタチオンペリオキシダーゼ）によって水になり解毒される。NO・と・$O_2^-$が反応するとONOO⁻となる。・OHは，ONOO⁻の分解によって，$H_2O_2$からFenton反応によって，あるいは，$H_2O_2$と・$O_2^-$からHaber-Weis反応によって生じる。

ことによって，細胞内のフリーラジカルや活性酸素種の量を定量することもできる。

　培養細胞の実験では，水素分子は，・$O_2^-$，$H_2O_2$，NO・を直接還元することはなく，・OHを消去し，培養細胞を酸化ストレスから保護した（図2）。

## 2. 水素分子の特徴と抗酸化剤 としての利点

　水素分子が，・$O_2^-$，$H_2O_2$，NO・を直接還元することはないという性質はきわめて重要である。・$O_2^-$，$H_2O_2$，NO・は，生体内でシグナルとして重要な役割をもつ。最近の大規模疫学調査によると，抗酸化剤の摂取し過ぎのヒトはむしろ短命であることが明らかにさ
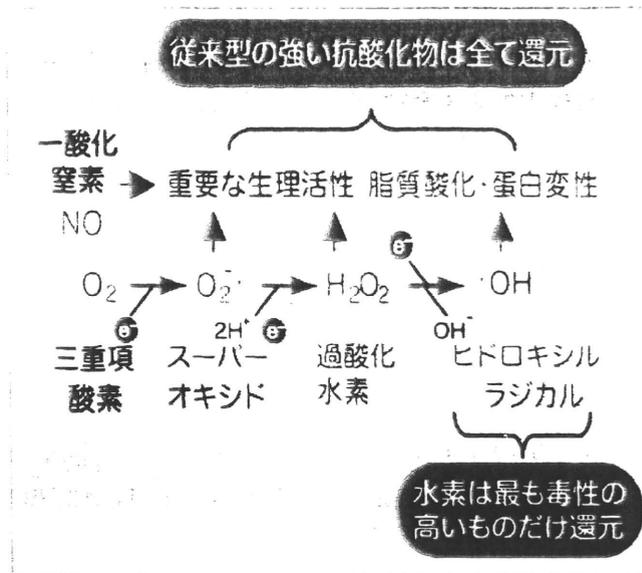
図2　活性酸素種の種類と性質。

　活性酸素種は，電子（e⁻）を吸収する毎に酸化力を増加させる。もっとも酸化力の強いヒドロキシルラジカル（・OH)は，水素分子と反応するが，その他の活性酸素種は水素分子とは反応しない。$H_2O_2$と・$O_2^-$は生体内シグナルとして重要な生理活性をもつので，これらの活性酸素種をすべて還元してしまうと副作用になる可能性がある。その点，水素分子は副作用が小さい（あるいは無い）と期待される。

れている。これは，・$O_2^-$，$H_2O_2$，・NOのような重要な生体内シグナルを消去してしまうからだと考えられている。すなわち，水素分子は，この点から考えて副作用がなさそうである。また，水素分子は体内に蓄積することはなく，容易に排出される。また，水素分子が酸化されて生じるのは水であり害はないはずである。

　もうひとつの水素分子の利点は，速い拡散性である。水素分子の拡散速度は速く細胞内にすみやかに浸透する。水素分子を溶解した点眼液を点眼すると眼球内に水素分子は拡散によって到達できるし，水素ガスを吸わせたラットでは，冠動脈の血流を停止させても水素分子が心筋内に到達することができることを実験的に証明している。

　さらに，水素分子の両親媒性という性質が利点である。多くの分子は，疎水性分子（油に溶けやすい分子）と親水性分子（水に溶けやすい分子）に分類される。水素分子は，イオン化せずに溶けており，水にも油にも同じ程度溶ける。細胞膜は脂質で構成され，細胞の中は基本的に水でできている。水素分子は，細胞膜を通過し細胞内に容易に到達し，核やミトコンドリアというオルガネラにも到達し，実際に酸化ストレスからミトコンドリアか核・遺伝子を護ることが証明されている。

## 3．水素分子の摂取法と体内への吸収

　水素分子は，水素ガス吸入することで体内にとりいれることができる。また，水素分子

を生理食塩水に溶解して静脈注射か腹腔注射によって注入する方法が動物実験で試みられている。水素ガスは腸内細菌が発生するので，腸内細菌を増やして水素ガスを発生させる試みもなされている。

　長期にわたって，水素分子を摂取する方法でもっとも簡便でしかも効果的なのは，水素水を飲用することである。水素水を飲むと水素分子は水と別個に挙動し体内に吸収される。水素分子のためのキャリアやトランスポーターがないことから（ないはずであるので）上皮を拡散で通過するらしい。実際に，水素水を動物の胃に入れると，血液に水素分子が検出されるし，肝臓や腎臓にも水素分子が検出される。血液の水素分子は，血液中の水素ガスを空気に放出させて，ガスクロマトグラフィーによって検出できるし，臓器の水素分子は水素電極で定量できる。

　あるいは，水素水を飲んだ後に呼気の水素ガスを定量できるので，水素分子は体内に取り込まれることがわかる。

## 4．水素水の安全性

　水素分子は，体温では安定な物質であり，触媒なしには酸素分子と反応することもない。水素分子は，我が国では1995年に食品添加物192番として厚生労働省で認可されており，度重なる安全性試験にパスしている。米国のNASAでも，水素分子のヒトに対する安全性が確認されている。

　水素ガスはすでに潜水病の予防と治療に用いられているという実績がある。高気圧で（深海で）血液に溶解した窒素ガスは気圧が下がると気泡になり，毛細血管を詰まらせる。それに対して，水素ガスは気泡になりにくいという性質があるので，その利点を生かした

ものである。

　すなわち，水素水の安全性は確認されており，水素水を販売することも承認されているので，一般への普及は容易であると考えられる。

## 5．水素水の動物実験

　水素ガスを吸引させた効果，水素分子溶解生理的食塩水や腸内細菌から発生させた水素ガスの効果は，別の機会に譲ることにし，水素水を動物に飲ませた実験結果を要約することにする。発表論文リストは，一般社団法人水素研究会のホームページに公表しているので，参考にしていただきたい。

http://www.hra-japan.org/paper3.html

①マウスを長期的に身体拘束すると脳に酸化ストレスが上昇し，認知機能が低下することが知られている。水素水を拘束期間中に飲ませると，脳の酸化ストレスが軽減し，認知機能の低下が抑制できた。

②apoEノックアウトマウスでは，動脈硬化が生じやすい。長期に水素水を飲ませると動脈硬化が抑制できた。

③抗がん剤のシスプラチンは腎臓の酸化ストレスを上昇させ，腎不全を生じさせる。水素水をマウスに自由摂取させると，シスプラチンの腎毒性が改善した。なお，シスプラチンの抗腫瘍効果は水素水によって低下しなかった。

④ビタミンC合成欠損マウスに水素水を与えると，虚血再灌流による脳の活性酸素種の発生が低下した。

⑤ラットに6-hydrodomamineを注入し脳の黒質領域を変性させ，パーキンソン病モデル動物を作製した。水素水の事前摂取のみならず，事後摂取においても改善効果を示

した。

⑥マウスにMPTPを投与し, パーキンソン病モデルを作製した。水素水自由摂取により改善効果を示した。

⑦水素水を飲用させることにより, マスト細胞の脱顆粒化を抑制し, 抗アレルギー作用を示した。

⑧拒絶反応を示すラット同士の腎臓移植後に, 水素水を飲用させると長期にわたって安定的に維持されることを示した。なお, 抗炎症マーカーが減少していた。

以上のように, 水素水は酸化ストレスに関連するモデル動物の症状を改善した。

共通の現象は, 抗酸化作用であり, さらに水素水の飲用によって, 抗炎症作用, 抗アレルギー作用もあることが判明した。

## 6. 分子機構の再考

上記のように培養細胞にヒドロキシルラジカルを発生させて, 水素分子が細胞を護ることを示したことから, 当初は, 水素分子が直接酸化力の強い活性酸素種やフリーラジカルを還元し, 細胞を酸化ストレスから護ることが想定された。培養細胞の場合は, 培養液に水素分子を飽和状態まで溶解させることができるので, それはそれで正しいと思われる。しかし, 水素水の自由摂取では, 摂取する水素分子の量は少なく, しかも短期間しか体内に維持できず, しかも, 当初の予測に反して, 飽和10%程度の低濃度でも効果があることがわかってきた。さらに, 抗炎症作用や抗アレルギー作用については, 直接の抗酸化剤というよりも水素分子がシグナルとして機能していることが伺える。

以上のような状況では, 少なくとも長期にわたって水素水を摂取させた時の効果は, 短時間の急性の酸化ストレス軽減効果とは別の機構が働いていることが示唆される。現在のところ, 水素分子の直接のターゲットは予想さえつかない。今後の研究によって, 少量の水素分子を長期にわたって摂取した時の効果のメカニズムを解明する必要がある。

## 7. 臨床試験

現在, 各地で水素水の臨床試験が開始されている。水素水の安全性が確認されていることから, 大学の倫理委員会の承認も得やすくなっている。筆者らが, 2007年に水素分子の論文を発表してから2年程度で, 臨床試験が積極的に開始されたのは, きわめて稀な例であり, 水素水への期待を物語っているものと思われる。

現在までに発表されている水素水の臨床効果は, 血液中の酸化ストレスマーカーの低下, 境界型糖尿病の糖負荷試験の改善, ミトコンドリア性糖尿病の血糖値(HbA1c)の低下, 皮膚/多発筋炎患者のアレルギーの指標MMP-3の低下などである。

近い将来には大規模臨床試験による水素水の効果が明確になることが期待される。

## 8. 水素水は老化を抑制できるか?

水素医学はまだはじまったばかりであり, めざましい進歩をとげている。水素分子の研究者たちが共通に口にするのは「正直, 当初は信じられなかったくらい水素分子の効果は著しい」ということである。水素水の抗酸化作用と抗炎症作用によって, 老化を抑制できる可能性は少なくない。

# Protection of the Retina by Rapid Diffusion of Hydrogen: Administration of Hydrogen-Loaded Eye Drops in Retinal Ischemia–Reperfusion Injury

*Hideaki Oharazawa,[1] Tsutomu Igarashi,[2] Takashi Yokota,[3] Hiroaki Fujii,[1] Hisaharu Suzuki,[2] Mitsuru Machide,[4] Hiroshi Takahashi,[2] Shigeo Ohta,[5] and Ikuroh Ohsawa[4]*

PURPOSE. Retinal ischemia-reperfusion (I/R) injury by transient elevation of intraocular pressure (IOP) is known to induce neuronal damage through the generation of reactive oxygen species. Study results have indicated that molecular hydrogen ($H_2$) is an efficient antioxidant gas that selectively reduces the hydroxyl radical ($\cdot OH$) and suppresses oxidative stress-induced injury in several organs. This study was conducted to explore the neuroprotective effect of $H_2$-loaded eye drops on retinal I/R injury.

METHODS. Retinal ischemia was induced in rats by raising IOP for 60 minutes. $H_2$-loaded eye drops were prepared by dissolving $H_2$ gas into a saline to saturated level and administered to the ocular surface continuously during the ischemia and/or reperfusion periods. One day after I/R injury, apoptotic cells in the retina were quantified, and oxidative stress was evaluated by markers such as 4-hydroxynonenal and 8-hydroxy-2-deoxyguanosine. Seven days after I/R injury, retinal damage was quantified by measuring the thickness of the retina.

RESULTS. When $H_2$-loaded eye drops were continuously administered, $H_2$ concentration in the vitreous body immediately increased and I/R-induced $\cdot OH$ level decreased. The drops reduced the number of retinal apoptotic and oxidative stress marker–positive cells and prevented retinal thinning with an accompanying activation of Müller glia, astrocytes, and microglia. The drops improved the recovery of retinal thickness by >70%.

CONCLUSIONS. $H_2$ has no known toxic effects on the human body. Thus, the results suggest that $H_2$-loaded eye drops are a highly useful neuroprotective and antioxidative therapeutic treatment for acute retinal I/R injury. (*Invest Ophthalmol Vis Sci.* 2010;51:487–492) DOI:10.1167/iovs.09-4089

Retinal ischemia-reperfusion (I/R) injury by transient elevation of intraocular pressure (IOP) in animal models is known to induce necrosis and apoptosis of cells and significant reductions in thickness in multiple layers of the retina.[1,2] Clinically, these features closely resemble several diseases such as acute angle-closure glaucoma, retinal artery occlusion, and amaurosis fugax.[3] It can irreversibly damage the retina, causing visual impairment and blindness. Immediate mechanisms of I/R injury involve the formation of reactive oxygen species (ROS),[4] which has been considered to contribute to the pathogenesis of many neurodegenerative diseases, including glaucomatous neurodegeneration.[5] Endogenous antioxidant enzymes and organic free radical scavengers can retard or prevent neuronal damages of retinal I/R injury in many animal models.[6-14] One highly reactive ROS, hydroxyl radical ($\cdot OH$), is generated during the early phase of reperfusion after ischemia and a major cause of retinal injury.[11-16] $\cdot OH$ attacks lipids, proteins and nucleic acids causing irreversible cellular damage.

In the past two decades, much attention has been focused on the use of several pharmaceutical gaseous molecules to attenuate oxidative stress.[17] A variety of gas delivery systems are used and under development for safe and effective administration of medical gases. We have reported that $H_2$ selectively reduces $\cdot OH$ and peroxynitrite without affecting other oxygen-derived free radicals.[18] Inhalation of $H_2$ gas has been demonstrated to limit the infarct volume of the brain, heart, and liver by reducing I/R injury[18-21] and can ameliorate intestinal transplant injury.[22] Moreover, the consumption of water with dissolved $H_2$ to a saturated level prevents stress-induced cognitive decline and 6-hydroxydopamine-induced nigrostriatal degeneration.[23,24] One clinical trial demonstrated a decrease in low-density lipoprotein after drinking $H_2$-loaded water.[25] $H_2$ has the potential to easily diffuse into organs and no known toxic effects on the human body.[18]

We have therefore developed a simple and effective method to deliver $H_2$ into lesions. The method is $H_2$-loaded eye drops, which are convenient, compared with the inhalation of $H_2$ gas, for the treatment of eye diseases. In this article, we demonstrate that the continuous administration of $H_2$-loaded eye drops immediately increases $H_2$ concentration in the vitreous body and prevents I/R-induced oxidative stress, leading to a decrease in apoptotic cell death in the retina and a decrease in retinal thinning with glial responses.

## METHODS

### Administration of $H_2$ and Measurement of Its Concentration

$H_2$-loaded eye drops were prepared by bubbling $H_2$ gas (flow rate: 1 L/min) through 400 mL of normal saline solution with stirring for 10 minutes to a saturated level (Fig. 1A), and then stored in an aluminum foil bag (Fig. 1B: Hosokawa Yoko, Tokyo, Japan) with no dead volume. The concentration of $H_2$ in the bag slowly decreased with a half-life of approximately 3 months. Freshly prepared $H_2$-loaded eye drops were administered to the ocular surface continuously (4 mL/min) with a dropper connected to the aluminum foil bag during the ischemia and/or reperfusion periods. The $H_2$ dissolved in saline solution was measured by using a needle-type $H_2$ sensor (Unisense, Aarhus N. Denmark). The $H_2$ concentration on the ocular surface was measured by touching the sensor to the surface. $H_2$ concentration was measured in the vitreous body by inserting the sensor into the vitreous body through the sclera.

To investigate the effect of $H_2$-loaded eye drops on retinal I/R injury, we applied them using four different time courses (see Fig. 4A): duration F, eye drop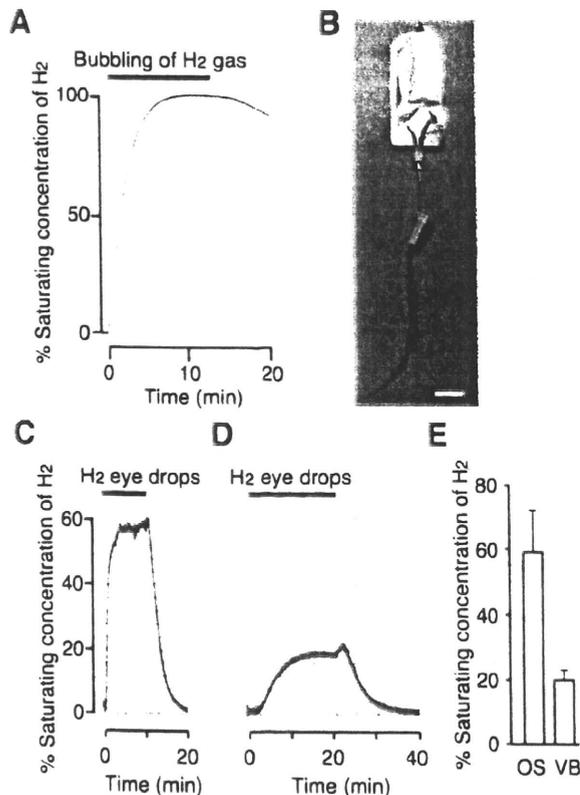s with and without $H_2$ were applied during an entire 90-minute process (60 minutes of ischemia followed by 30 minutes of reperfusion); duration I, eye drops with $H_2$ were applied only during ischemia; duration R, eye drops with $H_2$ were applied only after reperfusion; and duration I/R eye drops with $H_2$ were applied for 10 minutes before and 30 minutes after reperfusion.

### Induction of I/R Injury

Retinal I/R injury was induced essentially as described previously.[2,26] Seven-week-old male Sprague-Dawley rats weighing 200 to 250 g were anesthetized with an intraperitoneal injection of pentobarbital (100 mg/kg), and the pupils were dilated with topical phenylephrine hydrochloride and tropicamide. After topical application of 0.4% oxybuprocaine hydrochloride, the anterior chamber was cannulated with a 30-gauge infusion needle connected to a normal saline reservoir. The IOP was raised to 110 mm Hg for 60 minutes by elevating the saline reservoir. Body temperature was maintained at $37.0 \pm 0.5°C$ with a rectal thermometer probe and a heating pad during the experimental period. Retinal ischemia was confirmed by whitening of the iris and fundus. After 60 minutes of ischemia, the needle was withdrawn from the anterior chamber and the intraocular pressure was normalized. The animals were euthanatized with an overdose of anesthesia after reperfusion, and the eyes were immediately enucleated. All animals were treated in accordance with the ARVO Statement for the Use of Animals in Ophthalmic and Vision Research. The studies were approved by the Animal Care and Use Committee of Nippon Medical School. All experiments were performed by examiners blinded to the genotypes or treatments of the rat.

### Detection of ·OH

The procedure for the measurement of accumulated ·OH in the eye is similar to that previously described with modifications.[27] We used 2-[6-(4'-hydroxy)phenoxy-3H-xanthen-3-on-9-yl] benzoate (HPF; Daiichi Pure Chemicals, Tokyo, Japan), which detects highly reactive ROS including ·OH, as a fluorescence probe.[28] HPF (4 μL, 1 mM) was given intravitreally just before the induction of ischemia. Rats were killed after 60 minutes of ischemia followed by 15 minutes of reperfusion. Retinas were quickly removed and flat mounted without fixation. The fluorescence images were acquired by using a laser scanning confocal microscope. The acquired images were analyzed by quantitative comparisons of the relative fluorescence intensity of retinas between groups (NIH Image software, developed by Wayne Rasband, National Institutes of Health, Bethesda, MD, available at http://rsb.info.nih.gov/ij/index.html).

### Histopathologic and Morphometric Study

Eyes were enucleated 7 days after reperfusion and fixed in 1% glutaraldehyde and 4% paraformaldehyde (PFA) in 0.1 M phosphate-buffered saline (PBS) for 30 minutes, and the anterior segments were removed. Corneas and lenses were discarded. The entire eye cups were further fixed in the same solution overnight and then transferred to 30% sucrose for cryoprotection. Cryosections (10 μm thick) were cut along the vertical meridian of the eye, passing through the optic nerve head, and were stained with hematoxylin and eosin (H&E). Retinal damage was assessed by measuring the thickness of the retina.[1] The thickness is defined as the total width between the inner limiting membrane to the interface of the outer plexiform layer and the outer nuclear layer. These measurements were made at a distance within 1 to 2 mm from the optic disc using a light microscope. The value was averaged from four measurements in the temporal and nasal hemispheres of three different sections.

### TUNEL Assay and Immunohistochemical Staining

One day or 7 days after reperfusion, the eyes were immediately enucleated. For TUNEL assay and the staining of reactive gliosis markers, they were fixed in 4% PFA, and for staining of oxidative stress markers they were fixed in Bouin's fluid for 30 minutes. Next, the anterior



**FIGURE 1.** $H_2$-loaded eye drops increased intravitreal $H_2$. **(A)** $H_2$-loaded eye drops were prepared by bubbling $H_2$ gas (*solid thick line*, flow rate: 1 L/min) through 400 mL of normal saline solution. After the bubbling was stopped, the $H_2$ concentration was gradually decreased by stirring and reached <1% within 90 minutes. **(B)** $H_2$-loaded eye drops were stored in an aluminum foil bag and administered to the ocular surface with a dropper. Scale bar, 4 cm. The concentrations of $H_2$ on the ocular surface **(C)** and in the vitreous body **(D)** were monitored with a needle-type $H_2$ sensor. *Solid thick line*: application times of $H_2$-loaded eye drops (4 mL/min). **(E)** Summary data showing $H_2$ concentration on the ocular surface (OS; $n = 3$) and in the vitreous body (VB; $n = 3$). Data represent the mean $\pm$ SD.

segments were removed and the corneas and lenses were discarded. For the TUNEL assay and for the staining of reactive gliosis markers, the obtained entire eye cups were further fixed in the same solution overnight. For the staining of oxidative stress markers, they were further fixed in the same solution for 2 hours. After cryoprotection with 30% sucrose, cryosections (10 μm thick) were cut along the vertical meridian of the eye, passing through the optic nerve head. TUNEL staining was performed with an apoptosis detection kit according to the supplier's instructions (Chemicon, Norcross, GA).[29] The numbers of TUNEL-positive cells in the retina were counted at a final magnification ×200 for each section using a light microscope.

For the immunostaining of oxidative stress markers, 4-hydroxynonenal (4-HNE) and 8-hydroxy-2-deoxyguanosine (8-OHdG),[30,31] cryosections were postfixed in acetone and stained using the ABC kit according to the supplier's instructions (Vector Laboratories, Burlingame, CA).[18] Sections were incubated with the following primary antibodies: mouse monoclonal anti-4-HNE (1:400; JaICA, Shizuoka, Japan) and mouse monoclonal anti-8-OHdG (1:20; JaICA), in a blocking buffer for 1 hour at 4°C. The stained sections were further counterstained for nuclei with methyl green (0.5%). A light microscope was used to count the number of 4-HNE- and 8-OHdG-positive cells in each section of the retina at a final magnification of ×200.

For immunofluorescent staining of microglia and macroglia (astrocytes and Müller cells), cryosections were incubated with the following primary antibodies: rabbit polyclonal anti-Iba1[32] (1:100; Wako, Osaka, Japan) or rabbit polyclonal anti-glial fibrillary acidic proteins (GFAP; 1:500; DAKO, Glostrup, Denmark) in blocking buffer for 1 hour at room temperature. After they were washed twice with PBS, the sections were incubated with fluorescein isothiocyanate (FITC)-conjugated secondary antibody (1:100; Invitrogen, Carlsbad, CA) for 30 minutes and further counterstained for nuclei with propidium iodide for 10 minutes. A laser scanning confocal microscope (FV300; Olympus, Tokyo, Japan) was used to count the number of Iba1-positive cells in each section of the retina at a final magnification of ×200.

## Statistical Analysis

All data are presented as the mean ± SD. For single comparisons, we performed an unpaired two-tailed Student's *t*-test. For multiple comparisons, we used an analysis of variance (ANOVA) followed by the Fisher least-significant difference (LSD) test (StatView; SAS Institute Cary, NC). $P < 0.05$ was considered statistically significant.

## RESULTS

### Effect of H₂-Loaded Eye Drops on H₂ Concentration in the Vitreous Body and the Accumulation of ·OH during Retinal I/R

We prepared an H₂-saturated normal saline solution (0.8 mM, pH 7.2; H₂-loaded eye drops) and packed it into an aluminum foil bag to prevent a decrease in H₂ concentration. A dropper connected to the bag was held close to the rat's eye, and drops were applied to the ocular surface. The time-course of changes in H₂ levels was monitored with a needle-shaped hydrogen sensor electrode inserted through the sclera to the vitreous body. When H₂-loaded eye drops were administered continuously, approximately 0.5 mM H₂ was detected on the ocular surface (Fig. 1C). Two minutes after the start of administration, H₂ concentration in the vitreous body started to increase and reached a maximum level after 15 minutes (Fig. 1D). At that time, the H₂ concentration accounted for approximately 20% (0.16 mM) of the H₂-loaded eye drops. Immediately after administration of the H₂-loaded eye drops ceased, the H₂ concentration in the vitreous body was observed to gradually decrease and then completely disappear after 15 minutes (Fig. 1D). The maximum observed concentration of H₂ in the vitreous body

was approximately one third of that observed on the ocular surface (Fig. 1E)

To verify that the diffused H₂ protects against ·OH during retinal I/R, we assessed the accumulation of ·OH by the fluorescence signal emitted by the oxidized form of HPF.[28] We produced retinal ischemia in rats by increasing IOP with an infusion needle connected to a saline bag. Just before the induction of ischemia, 4 μL of 1 mM HPF was given intravitreally, followed by 60 minutes of ischemia. Fifteen minutes after reperfusion, the retinas were flatmounted and imaged in their entirety using a laser confocal-scanning microscope (Fig. 2A). The retinal HPF-fluorescence in the H₂-loaded eye drop-treated group was significantly less than that in the vehicle-treated group (Fig. 2B).

### Effect of H₂-Loaded Eye Drops on the Number of Apoptotic and Oxidative Stress Marker–Positive Cells

To determine whether the administration of H₂-loaded eye drops protects against retinal I/R injury, eye drops with and without H₂ were applied during the entire 90 minutes process (60 minutes of ischemia followed by 30 minutes of reperfusion). One day after I/R injury, a remarkable increase in the number of apoptotic cells (TUNEL-positive cells) was observed in both the inner and the outer nuclear layers of vehicle-treated retinas (Fig. 3A); however, the administration of H₂-loaded eye drops resulted in a significant decrease (approximately 77%, $P < 0.0001$) of TUNEL-positive cells (Figs. 3A, 3B), indicating that H₂-loaded eye drops had potent antiapoptotic activity. We speculate that the decreased apoptotic cell death reflects the H₂-dependent reduction of oxidative stress, which was mainly promoted by ·OH.

We then examined the levels of two oxidative stress markers, 4-HNE and 8-OHdG, in the vehicle-treated and the H₂-loaded eye drop–treated eyes by immunohistochemical staining with each specific antibody.[30,31] As expected,[9] 1 day after I/R injury, the number of 4-HNE- and 8-OHdG-positive cells increased dramatically in the retina (Figs. 3C, 3E, respectively). However, eyes that had been treated with H₂-loaded eye drops exhibited significantly fewer 4-HNE and 8-OHdG-positive cells compared with the vehicle-treated retinas (Figs. 3C–F), supporting our formulated hypothesis.
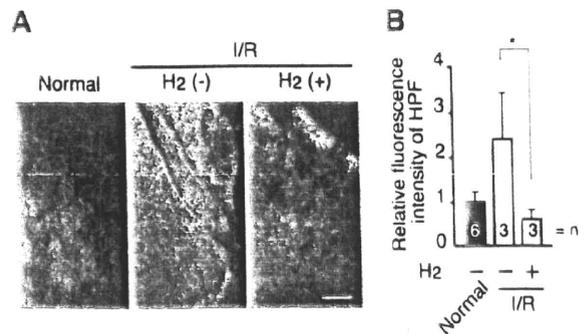


**FIGURE 2.** H₂-loaded eye drops reduced hydroxyl radicals in the retina. HPF was given intravitreally just before the induction of ischemia. After I/R, the retinas were quickly removed and flatmounted. (A) Representative fluorescent images were obtained with a laser scanning confocal microscope. (B) HPF fluorescence was quantified from the entire retina of each independent experiment. *$P < 0.01$. Data represent the mean ± SD. Scale bar, 200 μm.
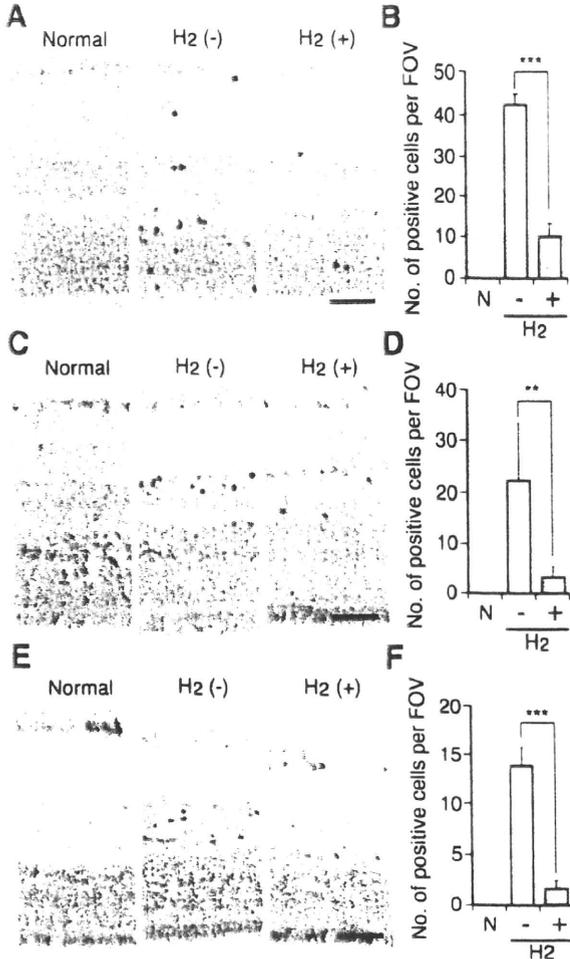
490 Oharazawa et al.

IOVS, January 2010, Vol. 51, No. 1



**FIGURE 3.** H$_2$-loaded eye drops reduced apoptotic cell death and oxidative stress. One day after I/R, the eyes were immediately enucleated and fixed for TUNEL assay (**A, B**) and staining with antibodies against oxidative stress markers 4-HNE (**C, D**) and 8-OHdG (**E, F**). Images of representative slices (**A, C, E**) and the number of positive cells per field of view (FOV) (**B, D, F**) in normal retina (N) and the I/R-injured retinas treated with the vehicle (H$_2$ −) or the H$_2$-loaded eye drops (H$_2$ +) are shown ($n$ = 5 animals per group). **P < 0.001, ***P < 0.0001. Data represent the mean ± SD. Scale bar, 30 μm.

## Effect of H$_2$-Loaded Eye Drops on Histopathologic and Morphometric Changes

To further evaluate the protective effect of H$_2$-loaded eye drops, we observed histopathologic and morphometric changes 7 days after retinal I/R injury. First, eye drops with and without H$_2$ were applied during the entire 90-minute process (duration F in Fig. 4A). Histopathologic changes of the retina at 7 days after I/R injury are depicted in Figure 4B. The H$_2$-loaded eye drop-treated group showed a nearly normal structure with a thicker retina; however, the H$_2$-free (vehicle) eye drops-treated group exhibited a marked thinning and atrophy of the retina. Quantitative morphometry of retinal thickness was used to estimate the effect of H$_2$ (Fig. 4C). The thickness in the I/R-injured retina treated with the H$_2$-loaded eye drops (102.6 ± 3.8 μm) increased significantly compared with the retina treated with the vehicle (66.9 ± 7.8 μm, P < 0.0001). In normal retina from untreated animals, the mean thickness of

the retina was 117.0 ± 4.5 μm, indicating that the H$_2$-loaded eye drops improved the recovery of retinal thickness by >70%.

To investigate the effect of different durations of H$_2$-loaded eye drop administration, we applied H$_2$-loaded eye drops using three different time courses (Fig. 4A) and observed that the H$_2$-loaded eye drops exerted their effect only when H$_2$ was already inside the eyeball at the onset of reperfusion (Fig. 4C). There were no significant differences in retinal thickness between groups treated with H$_2$-loaded eye drops only after reperfusion (duration R; 75.4 ± 10.4 μm) and treated with
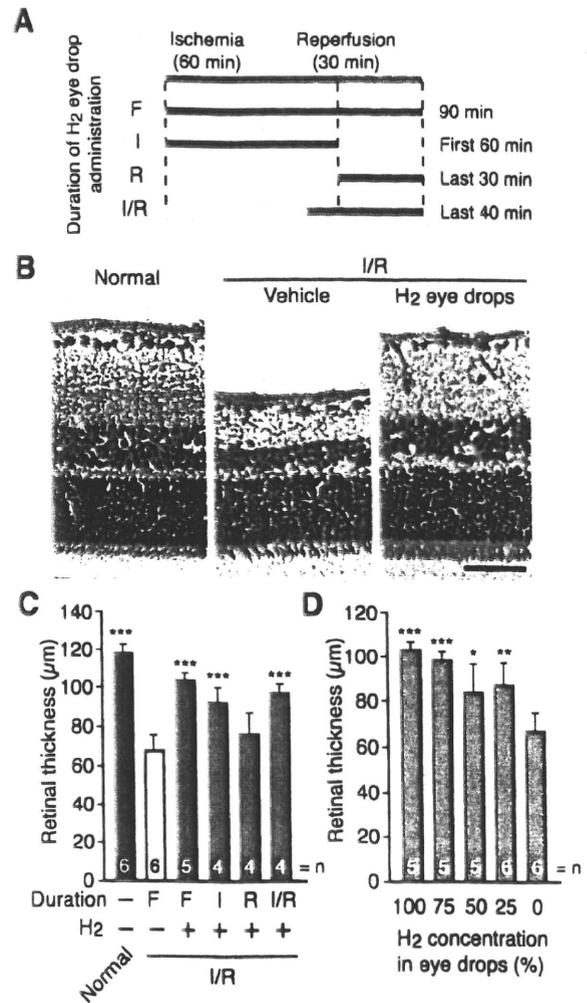


**FIGURE 4.** H$_2$-loaded eye drops prevented retinal degeneration caused by I/R. One week after I/R injury, the retinas were sliced and stained with H&E. (**A**) Schematic of the experiment, with four different durations of H$_2$-loaded eye drops administration. (**B**) Images of representative slices of normal retinas, I/R-injured retinas treated with vehicle and retinas treated with H$_2$-loaded eye drops during the entire 90-minute process (60 minutes of ischemia followed by 30 minutes of reperfusion) are shown. Scale bar, 50 μm. (**C**) Retinal thicknesses for different durations of H$_2$-loaded eye drops (100%) administration. ***P < 0.0001 compared with I/R-injured retina treated with the vehicle (H$_2$ −). (**D**) Retinal thicknesses at different concentrations of H$_2$ in eye drops. The retinas were treated with H$_2$-loaded eye drops during the entire process (duration F). *P < 0.01, **P < 0.001, ***P < 0.0001 compared with I/R-injured retina treated with 0% H$_2$. Histograms represent the mean ± SD.

vehicle ($P$ = 0.06). However, the retina that was treated with $H_2$-loaded eye drops only during ischemia (duration I; 91.6 ± 7.5 μm) was still significantly thicker than that treated with the vehicle ($P$ < 0.01). We next administered $H_2$-loaded eye drops for 10 minutes before and 30 minutes after reperfusion (duration I/R) and observed that the administration schedule was sufficient to suppress the reduction of retinal thickness (duration I/R; 96.6 ± 4.4 μm; $P$ < 0.001 vs. vehicle). Furthermore, we applied eye drops diluted to 25%, 50%, and 75% of the normal $H_2$-loaded eye drops during the entire 90-minute process and observed that $H_2$-loaded eye drops suppressed the reduction of retinal thickness in a dose-dependent manner (Fig. 4D). It is notable that the 25%-diluted $H_2$-loaded eye drops were still effective.

### Effect of $H_2$-Loaded Eye Drops on Glial Activation

Considering the critical role of increasing glial activation in the pathogenic progression of retinal damage, we investigated the immunohistochemical changes of the Iba1[32] and GFAP[33] at 7 days after retinal I/R injury with and without $H_2$ treatment. Iba1 is specifically expressed by microglia/macrophages.[34] A small number of Iba1-positive cells was observed in normal retinas, whereas an increasing number of Iba1-positive cells was observed in I/R-injured retinas. At that time, $H_2$-loaded eye drops were observed to inhibit the activation of microglia (Figs. 5A, 5B), indicating that the ongoing neurodegeneration, which activated microglia, was repressed by $H_2$. In addition, $H_2$-loaded eye drops repressed the increase in GFAP immunoreactivity in I/R-injured retinas. The only GFAP-positive cells in normal retina are astrocytes, whereas in the injured retinas, Müller cells, the specific glial cells in the retina, react with anti-GFAP antibody across the retinal layers.[33] In vehicle-treated retinas, GFAP was quite prominent in the Müller cells
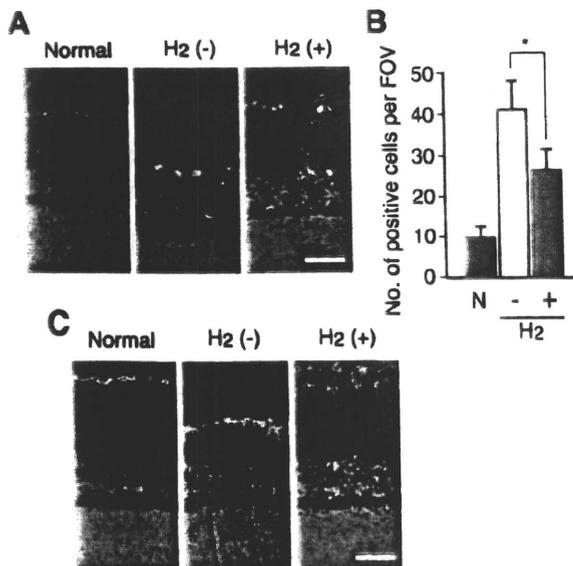
FIGURE 5. $H_2$-loaded eye drops prevented glial activation caused by I/R in the retina. One week after I/R injury, the retinas were sliced, stained with antibodies to Iba1 (a marker for microglia/macrophages, *green*) (A, B) and GFAP (a marker for Müller cells and astrocytes, *green*) (C), and further counterstained for nuclei with propidium iodide (*red*). Images of representative slices (A, C) and the number of positive cells per field of view (FOV) (B) in normal retina (N) and I/R-injured retinas treated with the vehicle ($H_2$ –) or $H_2$-loaded eye drops ($H_2$ +) are shown ($n$ = 5 animals per group). *$P$ < 0.01. Data represent the mean ± SD. Scale bar, 50 μm.

across the retinal layers and was also strongly present in the astrocytes of the nerve fiber layers, when compared with the $H_2$-loaded eye drop-treated retinas (Fig. 5C).

## DISCUSSION

$H_2$-loaded eye drops have a strong protective effect against retinal I/R injury. Previous studies have demonstrated that antioxidants can decrease retinal injury[6-15]; however, because antioxidants are difficult to deliver into the vitreous body by topical administration, they were injected into either the eye or the peritoneal cavity. Thus, easily applicable antioxidative reagents without significant side effects are strongly desirable. $H_2$ is an antioxidant that can easily diffuse into the body. We have observed that $H_2$ diffuses into the organelles, including mitochondria and the nucleus, of cultured cells.[18] These properties prompted us to attempt the administration of $H_2$-loaded eye drops for retinal diseases. This is the first report that $H_2$ can immediately penetrate the vitreous body after the administration of $H_2$-loaded eye drops, thereby directly reducing a toxic ROS, ·OH, which is produced during I/R. This effectively protects the retina from I/R injury.

Although the sources and mechanisms of ROS generation during I/R by transiently raised IOP are not clearly understood, ROS kills neurons in the ganglion cell layer, inner nuclear layer, and outer nuclear layer mainly by apoptosis.[5,9,35] Ophir et al.[14,15] demonstrated that a burst of ·OH occurs in the cat retina during the early reperfusion phase (5 minutes of reperfusion). Thus, we assessed ·OH after 15 minutes of reperfusion with HPF fluorescence and found that the accumulation of ·OH was reduced by $H_2$-loaded eye drops in the I/R-injured retina, indicating that $H_2$ directly reduced ·OH and decreased subsequent oxidative stress. Indeed, 1 day after reperfusion, $H_2$-loaded eye drops dramatically decreased 4-HNE-, 8-OHdG-, and TUNEL-positive cells indicating that $H_2$ protected lipids from peroxidation and DNA from oxidation and reduced subsequent retinal cell death (detected as apoptosis) after I/R injury.

Neurodegeneration was obvious at 7 days after retinal I/R injury. Previous studies on retinal damage 7 days after I/R injury have shown that the thinning of the retina was evident both morphologically and morphometrically.[1,36,56,57] In the present study, $H_2$-loaded eye drops clearly suppressed the thinning of the retina. However, when $H_2$-loaded eye drops were applied after the onset of reperfusion (duration R), they did not protect from retinal damage (Fig. 4). As shown in Figure 1, $H_2$ concentration in the vitreous body gradually increased after 2 minutes and reached its maximum level after 15 minutes. Immediately after $H_2$-loaded eye drop administration was stopped, the $H_2$ level gradually decreased and then completely disappeared after 15 minutes. Thus, $H_2$ applied after the onset of reperfusion could not reach a level sufficient to inhibit the accumulation of ·OH in the early reperfusion phase, whereas $H_2$ applied before or during reperfusion (duration I or I/R) had a high enough $H_2$ level.

Microglia, Müller cells, and most likely astrocytes respond within hours to elevation of IOP in the retina.[38] Heterogeneous populations of microglia/macrophages are observed in the normal retina and activated early after I/R injury.[39] Dying neurons are phagocytosed by them. The long duration of ROS production (up to 48 hours after I/R) may be explained partly by the infiltration of microglia/macrophages into the site of inflammation.[7] The presence of GFAP in a glial cell is considered a marker for reactive gliosis, which is not neuroprotective but rather promotes neurodegeneration.[40] $H_2$-loaded eye drops reduced the number of reactive glia, indicating that $H_2$-loaded eye drops during I/R were sufficient to suppress harmful gliosis after I/R injury and recover the thickness of the retina.

In conclusion, this study demonstrates that the topical application of $H_2$ can be a useful antioxidant to protect against retinal I/R injury by direct $H_2$ diffusion into the retina. Accordingly, this neuroprotective antioxidant could offer a new therapeutic strategy to the clinical setting to reduce retinal damage in acute glaucoma and acute retinal vascular occlusion.

## References

1. Hughes WF. Quantitation of ischemic damage in the rat retina. *Exp Eye Res.* 1991;53:573-582.
2. Kuroiwa S, Katai N, Shibuki H, et al. Expression of cell cycle-related genes in dying cells in retinal ischemic injury. *Invest Ophthalmol Vis Sci.* 1998;39:610-617.
3. Osborne NN, Casson RJ, Wood JPM, Chidlow G, Graham M, Melena J. Retinal ischemia: mechanisms of damage and potential therapeutic strategies. *Prog Retina Eye Res.* 2004;23:91-147.
4. McCord JM. Oxygen-derived free radicals in postischemic tissue injury. *N Engl J Med.* 1985;312:159-163.
5. Tezel G. Oxidative stress in glaucomatous neurodegeneration: mechanisms and consequences. *Prog Retinal Eye Res.* 2006;25: 490-513.
6. Szabo ME, Droy-Lefaix MT, Doly M, Carré C, Braquet P. Ischemia and reperfusion-induced histologic changes in the rat retina. *Invest Ophthalmol Vis Sci.* 1991;32:1471-1478.
7. Muller A, Pietri S, Villain M, Frejaville C, Bonne C, Culcasi M. Free radicals in rabbit retina under ocular hyperpressure and functional consequences. *Exp Eye Res.* 1997;64:637-643.
8. Shibuki H, Katai N, Kuroiwa S, Kurokawa T, Yodoi J, Yoshimura N. Protective effect of adult T-cell leukemia-derived factor on retinal ischemia-reperfusion injury in the rat. *Invest Ophthalmol Vis Sci.* 1998;39:1470-1477.
9. Shibuki H, Katai N, Yodoi J, Uchida K, Yoshimura N. Lipid peroxidation and peroxynitrite in retinal ischemia-reperfusion injury. *Invest Ophthalmol Vis Sci.* 2000;41:3607-3614.
10. Hirooka K, Miyamoto O, Jinming P, et al. Nueroprotective effects of D-allose against retinal ischemia-reperfusion injury. *Invest Ophthalmol Vis Sci.* 2006;47:1653-1657.
11. Zhang B, Safa R, Rusciano D, Osborne NN. Epigallocatechin gallate, an active ingredient from green tea, attenuates damaging influences to the retina caused by ischemia/reperfusion. *Brain Res.* 2007;1159:40-53.
12. Peachey NS, Green DJ, Ripps H. Ocular ischemia and the effects of allopurinol on functional recovery in the retina of the arterially perfused cat eye. *Invest Ophthalmol Vis Sci.* 1993;34:58-65.
13. Li S, Fu Z, Ma H, et al. Effect of lutein on retinal neurons and oxidative stress in a model of acute retinal ischemia/reperfusion. *Invest Ophthalmol Vis Sci.* 2009;50:836-843.
14. Ophir A, Berenshtein E, Kitrossky N, et al. Hydroxyl radical generation in the cat retina during reperfusion following ischemia. *Exp Eye Res.* 1993;57:351-357.
15. Ophir A, Berenshtein E, Kitrossky N, Averbukh E. Protection of the transiently ischemic cat retina by zinc-desferrioxamine. *Invest Ophthalmol Vis Sci.* 1994;35:1212-1222.
16. Song Y, Gong Y, Xie Z, Li C, Gu Q, Wu X. Edaravone (MCI-186), a free radical scavenger, attenuates retinal ischemia/reperfusion injury in rats. *Acta Pharmacol Sin.* 2008;29:823-828.
17. Nakao A, Sugimoto R, Billiar TR, McCurry KR. Therapeutic antioxidant medical gas. *J Clin Biochem Nutr.* 2009;44:1-13.
18. Ohsawa I, Ishikawa M, Takahashi K, et al. Hydrogen acts as a therapeutic antioxidant by selectively reducing cytotoxic oxygen radicals. *Nat Med.* 2007;13:688-694.
19. Cai J, Kang Z, Liu K, et al. Neuroprotective effects of hydrogen saline in neonatal hypoxia-ischemia rat model. *Brain Res.* 2009; 1256:129-137.
20. Hayashida K, Sano M, Ohsawa I, et al. Inhalation of hydrogen gas reduces infarct size in the rat model of myocardial ischemia-reperfusion injury. *Biochem Biophys Res Commun.* 2008;373:30-35.
21. Fukuda K, Asoh S, Ishikawa M, Yamamoto Y, Ohsawa I, Ohta S. Inhalation of hydrogen gas suppresses hepatic injury caused by ischemia/reperfusion through reducing oxidative stress. *Biochem Biophys Res Commun.* 2007;361:670-674.
22. Buchholz BM, Kaczorowski DJ, Suquimoto R, et al. Hydrogen inhalation ameliorates oxidative stress in transplantation induced intestinal graft injury. *Am J Transplant.* 2008;8:2015-2024.
23. Nagata K, Nakashima-Kamimura N, Mikami T, Ohsawa I, Ohta S. Consumption of molecular hydrogen prevents the stress-induced impairments in hippocampus-dependent learning tasks during chronic physical restraint in mice. *Neuropsychopharmacology.* 2009;34:501-508.
24. Fu Y, Ito M, Fujita Y, et al. Molecular hydrogen is protective against 6-hydroxydopamine-induced nigrostriatal degeneration in a rat model of Parkinson's disease. *Neurosci Lett.* 2009;453:81-85.
25. Kajiyama S, Hasegawa G, Asano M, et al. Supplementation of hydrogen-rich water improves lipid and glucose metabolism in patients with type 2 diabetes or impaired glucose tolerance. *Nutr Res.* 2008;28:137-143.
26. Lam TT. The effect of 3-aminobenzamide, an inhibitor of poly-ADP-ribose polymerase, on ischemia/reperfusion damage in rat retina. *Res Commun Mol Pathol Pharmacol.* 1997;95:241-252.
27. Tomizawa S, Imai H, Tsukada S, et al. The detection and quantification of highly reactive oxygen species using the novel HPF fluorescence probe in a rat model of focal cerebral ischemia. *Neurosci Res.* 2005;53:304-313.
28. Setsukinai K, Urano Y, Kakinuma K, Majima HJ, Nagano T. Development of novel fluorescence probes that can reliably detect reactive oxygen species and distinguish specific species. *J Biol Chem.* 2003;278:3170-3175.
29. Gavrieli Y, Sherman Y, Ben-Sasson SA. Identification of programmed cell death in situ via specific labeling of nuclear DNA fragmentation. *J Cell Biol.* 1992;119:493-501.
30. Petersen DR, Doorn JA. Reactions of 4-hydroxynonenal with proteins and cellular targets. *Free Radic Biol Med.* 2004;37:937-945.
31. Kamiya H. Mutagenicities of 8-hydroxyguanine and 2-hydroxyadenine produced by reactive oxygen species. *Biol Pharm Bull.* 2004;27:475-479.
32. Imai Y, Ibata I, Ito D, Ohsawa K, Kohsaka S. A novel gene iba 1 in the major histocompatibility complex class III region encoding an EF hand protein expressed in a monocytic lineage. *Biochem Biophys Res Commun.* 1996;224:855-862.
33. Block F, Grommes C, Kosinski C, Schmidt W, Schwarz M. Retinal ischemia induced by the intraluminal structure method in rats. *Neurosci Lett.* 1997;232:45-48.
34. Sasaki Y, Ohsawa K, Kanazawa H, et al. Iba1 is an actin-cross-linking protein in macrophages/microglia. *Biochem Biophys ResCommun.* 2001;286:292-297.
35. Bonne C, Muller A, Villain M. Free radicals in retinal ischemia. *Gen Pharmac.* 1998;30:275-280.
36. Takahashi K, Lam TT, Edward DP, Buchi ER, Tso MOM. Protective effects of flunarizine on ischemic injury in the rat retina. *Arch Ophthalmol.* 1992;110:862-870.
37. Junk AK, Mammis A, Savitz SI, et al. Erythropoietin administration protects retinal neurons from acute ischemia-reperfusion injury. *Proc Natl Acad Sci USA.* 2002;99:10659-10664.
38. Wang X, Tay SS, Ng YK. An immunohistochemical study of neuronal and glial cell reactions in retinae of rats with experimental glaucoma. *Exp Brain Res.* 2000;132:476-484.
39. Zhang C, Lam TT, Tso MO. Heterogeneous populations of microglia/macrophages in the retina and their activation after retinal ischemia and reperfusion injury. *Exp Eye Res.* 2005;81:700-709.
40. Kim K, Ju W, Neufeld AH. Neuronal susceptibility to damage: comparison of the retinas of young, old and old/caloric restricted rats before and after transient ischemia. *Neurobiol Aging* 2004; 25:491-500.

Contents lists available at ScienceDirect

# Behavioural Brain Research

Research report

# Regular voluntary exercise cures stress-induced impairment of cognitive function and cell proliferation accompanied by increases in cerebral IGF-1 and GST activity in mice

Sanae Nakajima[a], Ikuroh Ohsawa[a], Shigeo Ohta[a], Makoto Ohno[b], Toshio Mikami[c],*

[a] Department of Biochemistry and Cell Biology, Institute of Gerontology, Nippon Medical School, Kawasaki, Kanagawa 211-8533, Japan
[b] Department of Graduate School of Nippon Sport Science University, 7-1-1 Fukasawa, Setagaya-ku, Tokyo 158-8508, Japan
[c] Department of Health and Sports Science, Nippon Medical School, 2-297-2 Kosugi-cho, Nakahara-ku, Kawasaki, Kanagawa 211-0063, Japan

## ARTICLE INFO

## ABSTRACT

Chronic stress impairs cognitive function and hippocampal neurogenesis. This impairment is attributed to increases in oxidative stress, which result in the accumulation of lipid peroxide. On the other hand, voluntary exercise enhances cognitive function, hippocampal neurogenesis, and antioxidant capacity in normal animals. However, the effects of voluntary exercise on cognitive function, neurogenesis, and antioxidants in stressed mice are unclear. This study was designed to investigate whether voluntary exercise cures stress-induced impairment of cognitive function accompanied by improvement of hippocampal neurogenesis and increases in antioxidant capacity. Stressed mice were exposed to chronic restraint stress (CRS), which consisted of 12 h immobilization daily and feeding in a small cage, for 8 weeks. Exercised mice were allowed free access to a running wheel during their exposure to CRS. At the 6th week, cognitive function was examined using the Morris water maze (MWM) test. Daily voluntary exercise restored stress-induced impairment of cognitive function and the hippocampal cell proliferation of newborn cells but not cell survival. Voluntary exercise increased insulin-like growth factor 1 (IGF-1) protein and mRNA expression in the cerebral cortex and liver, respectively. In addition, CRS resulted in a significant increase in the number of 4-hydrosynonenal (4-HNE)-positive cells in the hippocampal dentate gyrus; whereas, voluntary exercise inhibited it and enhanced glutathione s-transferases (GST) activity in the brain. These findings suggest that voluntary exercise attenuated the stress-induced impairment of cognitive function accompanied by improvement of cell proliferation in the dentate gyrus. This exercise-induced improvement was attributed to exercise-induced enhancement of IGF-1 protein and GST activity in the brain.

## 1. Introduction

Aging impairs cognitive functions such as learning and memory. Age-dependent impairment of cognitive function is accelerated by chronic stress, especially psychological stress, in humans. To elucidate the mechanism by which chronic stress impairs cognitive function, many studies on animals using stress models have been performed. In animal experiments, the most commonly used method for exposing animals to chronic stress is to restrict the physical activity of the animals by immobilization. Chronic restraint stress (CRS) caused by immobilization impairs cognitive function [1–3]. Furthermore, in Alzheimer's disease model mice over expressing human APP-CT100, CRS accelerates cognitive impairment, as assessed by the passive avoidance test and the

social tranche of the food preference test [4]. We also showed that CRS, which involves immobilization and feeding in a small cage, leads to impairment of cognitive function [5].

One of the factors attributed to stress-induced impairment of cognitive function is decreased neurogenesis, especially neurogenesis in the hippocampal dentate gyrus. Restrained rats (4 h/day for 7 days) show lower levels of hippocampal neurogenesis as estimated by the number of bromodeoxyuridine (BrdU)-positive cells compared with control mice [6]. Two weeks of CRS decreased hippocampal cell proliferation and the expression of brain-derived neurotrophic factor (BDNF) [7]. We also showed that CRS decreases hippocampal neurogenesis [5,8].

The mechanism through which CRS suppresses hippocampal neurogenesis has not been clearly elucidated; however, free radical formation induced by CRS is regarded as an important factor. CRS increases lipid peroxide [5,9,10] and protein carbonyl content [9] and the number of 4-hydroxynoneral (4-HNE)-positive cells [5,8]. Administration of hydrogen water [5], which acts as an

* Corresponding author. Tel.: +81 44 733 3719; fax: +81 44 733 3719.
E-mail address: mikami@nms.ac.jp (T. Mikami).

efficient antioxidant, or GliSODin [8], which enhances superoxide dismutase (SOD) activity by oral administration, attenuates stress-induced impairment of neurogenesis accompanied by a reduction in lipid peroxidation. In addition, regular exercise enhances SOD, the main antioxidant enzyme in vivo, activity in the liver [11] and heart [12], and exercise training increases glutathione s-transferase (GST) activity in the liver [13]. GST plays an important role in the exclusion of 4-HNE from cells [14,15]. These findings have led us to suppose that regular exercise attenuates hippocampal neurogenesis by enhancing cerebral antioxidant enzyme activity in stressed animals; however, this idea has not been confirmed yet.

On the other hand, there are many reports that positively influenced by running wheel exercise as enhanced hippocampus dependent learning [16–19]. Moreover, regular exercise improves cognitive function in aged mice [20] and transgenic mice with neuronal degeneration such as Alzheimer's disease [21,22] or Parkinson's disease [23] accompanied by an improvement in hippocampal neurogenesis.

One of the important which exercise improves cognitive function and hippocampal neurogenesis is to increase insulin-like growth factor 1 (IGF-1) uptake in the brain [24]. Exercise-induced improvement of hippocampal neurogenesis is cancelled out by inhibition of IGF-1 action using neutralizing antibodies [25]. However, it has been not reported whether regular exercise cures stress-induced impairment of cognitive function and hippocampal neurogenesis accompanied by the upregulation of the IGF-1 signaling pathway.

The purpose of this study was to investigate whether exercise cures stress-induced impairment of cognitive function and hippocampal neurogenesis, and, if so, we proposed to elucidate whether this beneficial effect of exercise is related to the IGF-1 signaling pathway or antioxidant capacity of the brain.

Our findings suggest that voluntary exercise attenuates stress-induced impairment of cognitive function accompanied by improvement of cell proliferation in the dentate gyrus. This exercise-induced improvement was attributed to exercise-induced enhancement of IGF-1 protein and GST activity in the brain.

## 2. Materials and methods

### 2.1. Animals and diet

All experimental procedures and animal treatments were performed in accordance with the guidelines of the laboratory animal manual of Nippon Medical School. Male C57/BL6 mice (Sankyo Lab Service, Tokyo, Japan), aged 7 weeks and that weighed 22.1 ± 1.3 g, were used. The mice were randomly divided into three groups: control mice (C mice; $n = 12$), restraint-stressed mice (RS mice; $n = 10$), and voluntary exercise mice (VE mice; $n = 9$). The C mice were housed in a standard mouse cage (width: 32 cm, length: 21.5 cm, height: 10.5 cm). In this case, four mice were housed per cage. The RS mice were housed in a cage divided into six cells. The divided cage was made by dividing a standard mice cage into six partitions with plastic boards to make the living space of the mice narrow [8]. In this cage, the living space per mouse was 10 cm wide, 10 cm long, and 10.5 cm tall. The VE mice were housed in a clear polycarbonate cage (width: 22 cm, length: 14 cm, height: 22 cm) with a free wheel (diameter: 17 cm) equipped with an electrical counter to measure the daily revolutions of a running wheel. All mice were fed with ad libitum access to food (standard animal diet) and tap water under a 12-h light/dark cycle (room temperature: 24 °C, 50% humidity).

### 2.2. Immobilization

After acclimation to the cage and diet for 5 days, the RS and VE mice were exposed to 12 h (a.m. 9:00–p.m. 9:00) of immobilization in an immobilization cage (width: 3 cm, length: 3 cm, height: 7.5 cm) 6 days a week for 5 weeks (Fig. 1). During daily immobilization, the mice were freely able to drink tap water.

### 2.3. Spatial learning and memory

After 5 weeks of chronic immobilization, the spatial memory of the mice was evaluated using the method of Morris water maze (MWM) test [26] modified by Carro et al. [24]. Briefly, the mice were trained for four trials a day for 5 days. A circular pool with a diameter of 115 cm was filled with water 1.5 cm above the plastic plat-
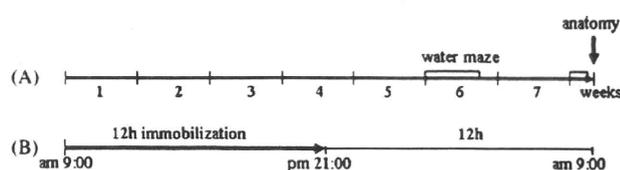


**Fig. 1.** Experimental protocol. (A) Total schedule. After 5 weeks of chronic immobilization, spatial memory of all mice was evaluated with Morris water maze test. (B) Daily schedule. RS and VE mice were exposed to 12 h of immobilization in a small cage at a frequency of 6 days per week and during 5 weeks. During the rest of day, RS and VE mice were housed in six-divided cage or clear polycarbonate cage with a free wheel, respectively.

form to hide it. The water was made opaque with white nontoxic paint, and the water temperature was set at 24 °C. A mouse was released into the pool facing the pool wall from four different starting points, which were varied randomly each day. The time taken to reach the platform (escape latency) was recorded for every trial. Each trial lasted either until the mouse had found the platform or for a maximum of 60 s. In each trial, the mice were allowed to rest on the platform for 20 s at the end of each trail. To determine long-term retention (memory), the MWM test was performed again on the 15th and 16th days after the first day of the MWM test (Fig. 1A).

### 2.4. 5-Bromodeoxyuridine (BrdU) injection

In the 5th week, BrdU dissolved in sterilized saline was intraperitoneally injected into all mice at 50 mg/kg body weight for four consecutive days.

### 2.5. Sample collection

The day after completion of the MWM test, the mice were anesthetized with pentobarbital and transcardially perfused with 60 ml of saline into their left ventricle. Their brains were carefully removed, and the hemispheres were separated. The left hemisphere was fixed in 4% paraformaldehyde in 0.1 M phosphate-buffered saline (PBS; 137 mM NaCl, 8.10 mM $Na_2HPO_4$, 2.68 mM KCl, 1.47 mM $KH_2PO_4$, pH 7.4) overnight at room temperature. After being washed three times with PBS, the brain was cut rostro-caudally with a Leica vibratome (VT 1000S, Leica Microsystems, Germany) at 40 μm. Serial sections were immersed in PBS. Ninety-six well plates were used to maintain the correct order of the sections in PBS at 4 °C. The right hemisphere was divided into the hippocampus, cerebral cortex, hypothalamus, and cerebellum. These samples were quickly frozen in liquid nitrogen and stored at −80 °C until analysis.

### 2.6. 4-HNE immunohistochemistry

To investigate lipid peroxidation in the hippocampus, 4-HNE immunohistochemistry was performed using an M.O.M. immunodetection kit (Vector laboratory, USA) according to the manufacturer's instructions. Briefly, free-floating sections were washed with PBS and reacted with 3% hydrogen peroxide in methanol for 30 min to block endogenous peroxidase activity. After being washed with PBS, the sections were exposed to heat (100 °C) in 100 mM citric acid buffer (pH 6.0) for 5 min using a microwave for antigen retrieval. After being washed again with PBS, the sections were incubated with M.O.M. mouse IgG blocking solution for 1 h at room temperature. After being washed with PBS, the sections were incubated with 10 μg/ml of monoclonal anti-4-HNE antibody (Japan Institute for the Control of Aging, Japan) in M.O.M diluent (0.1 M PBS; pH 7.4, 0.5% Triton X-100, 8% protein concentrate stock solution) for two nights at 4 °C with gentle shaking. After being washed with PBS, the sections were incubated with biotinylated anti-mouse IgG in M.O.M diluent (1:250) for 2 h at room temperature. After being washed with PBS, the sections were incubated with avidin–biotin–horseradish peroxidase complex for 2 h at room temperature. Finally, the sections were washed with PBS and developed using 0.67 mg/ml 3′3 diaminobenzidine (DAB) for 5 min. The sections were mounted, dehydrated, and cover slipped using permount mounting medium. The number of 4-HNE positive cells in the granule cell layer (GCL) was determined using a light microscope (ECLIPSE E400 Nikon; Nikon, Japan).

### 2.7. BrdU and Ki67 immunohistochemistry

BrdU- or Ki67-positive cells were identified immunohistochemically. The sections were incubated with 3% hydrogen peroxide in methanol to block endogenous peroxidase activity. BrdU sections were incubated with 2 M HCl for 30 min at 37 °C and M.O.M mouse IgG blocking solution for 1 h. Ki67 sections were subjected to the antigen retrieval reaction and blocked via non-specific staining with normal goat serum. After being washed with PBS, the sections were incubated for two nights with the primary antibody, a monoclonal anti-BrdU antibody (BD Pharmingen, 1:200) or rabbit polyclonal anti-Ki67 antibody (Abcam, 1:500), respectively. After being washed, the BrdU or Ki67 stained sections were incubated with anti-mouse biotinylated IgG secondary antibody (Vector Laboratories, 1:250) or goat anti-rabbit biotinylated IgG (Vector Laboratories, 1:100) for 2 h at room temperature, respectively. Both the BrdU and Ki67 sections were incubated with VECTASTAIN ABC

reagent (Vector Laboratories) for 90 min and developed using DAB. The number of BrdU- or Ki67-positive cells in the subgranular zone (SGZ) was determined using a light microscope.

### 2.8. Isolation of total RNA and real-time quantitative RT-PCR

Total RNA was isolated using the RNeasy Mini Kit (QIAGEN, Germany) according to the manufacturer's instructions. RNA quantification was carried out by measuring absorption at 260 nm. cDNA was generated from total RNA by reverse transcription (RT) using oligo $(dT)_{12-18}$ primers (Invitrogen, USA) and Superscript reverse transcriptase (Invitrogen, USA) in PCR terminal cycler DICS (Takara, Japan). The RT step consisted of 37 °C for 10 min and 50 °C for 60 min. The level of IGF-1 mRNA in the liver was measured by real-time quantitative PCR. Glyceraldhyde-3-phosphate dehydrogenase (GAPDH) served as an endogenous control. Quantification of the TaqMan® real-time PCR results was performed by plotting fluorescent signal intensity against the number of PCR cycles on a semi-logarithmic scale. The fluorescent probes and the forward and reverse primers were designed and synthesized by Hokkaido System Science (Hokkaido System Science Co., Ltd., Japan). The primer and probe sequences were as follows: Probe: GGCTTTTAC TTCAACAAGCCCAC-AGGCTATG, forward primer: TGGATGCTCTTCAGT-TCGTGTG, reverse primer: GCCTGTCTGAGG-GTGCCCTC. The reaction protocol for real-time PCR consisted of 50 °C for 5 min followed by 95 °C for 5 min. Forty cycles of a two-step PCR reaction consisting of 20 s at 95 °C and 1 min at 60 °C were performed. The real-time PCR values for IGF-1 were corrected relative to the values for glyceraldehyde-3-phosphate dehydrogenase (GAPDH).

### 2.9. ELISA for IGF-1

The level of IGF-1 in the cerebral cortex was assayed using an enzyme-linked immunosorbent assay (ELISA) for murine IGF-1 with anti-mouse IGF-1 antibodies (MAP791 and BAF791, R&D, USA) and mouse IGF-1 (IBT, Germany) as a standard (the sensitivity of the assay was 0.5 ng/ml) according to the manufacturer's instructions with IGF-1 antibodies.

### 2.10. Analysis of SOD and GST activity

SOD activity was measured using an SOD Assay Kit-WST (Dojindo Molecular Technologies Co, Tokyo). In brief, 20 mg of hippocampus were homogenized in a dilution buffer included in the SOD assay kit and centrifuged at 18,000 × g for 10 min. The protein concentration of the supernatant was measured using the Coomassie Plus Protein Assay Reagent Kit (Pierce CO. LTD, USA). The supernatant (20–50 μg protein) was used for measurement of SOD activity in accordance with the manufacturer's instructions. GST activity in the cerebral cortex was measured by the method of Habig et al. [27]. SOD and GST activity were expressed as units per gram of protein (units/g protein).

### 2.11. HPLC for α-tocopherol

The level of (-tocopherol in the hypothalamus was determined by high performance liquid chromatography (HPLC) according to the method of Milne et al. with some modifications [28]. We used the hypothalamus for α-tocopherol analysis because the hippocampus and cerebral cortex had already been used for other analyses.

## 3. Statistical analysis

All values are shown as the mean ± standard error of measurement (SEM). Differences between groups were analyzed using one- or two-way ANOVA. When statistical differences were found, Fisher's PLSD post hoc test was performance. Statistical significance was accepted as $p < 0.05$. All the experiments were examined in a blinded fashion.

## 4. Results

### 4.1. Changes in the running distance of the VE mice

The running distance of each VE mouse was calculated by multiplying the wheel diameter (17 cm) by the VER. The running distance of the VE mice gradually decreased in the latter half of the experiment. The mean running distance of the VE mice was 5.8 ± 2.0 km/day (Fig. 2).

### 4.2. Learning and memory

To examine whether CRS influences cognitive function, we tested both learning and memory using the MWM test (Fig. 3).
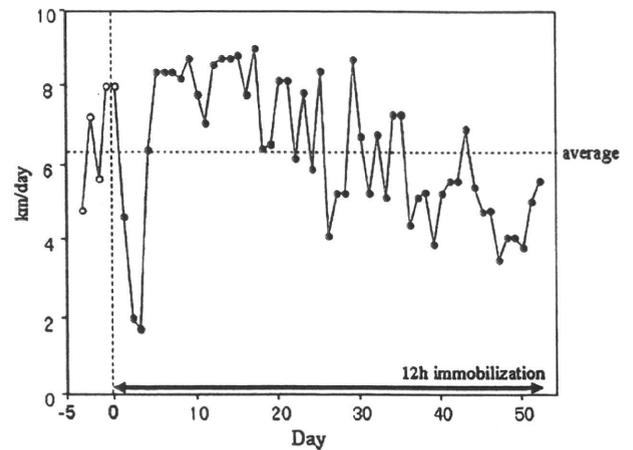


Fig. 2. Change of running distance in VE mice. Running distances performed by the VE mice housed in a cage equipped with a free wheel gradually decreased in the latter period of the experiment.

For learning, the C mice showed a gradual curtailment of the time taken to find the hidden platform, referred to as the latency from hereon in, during the 5 day training period; whereas, the RS and VE mice showed a smaller reduction of latency and a significantly longer latency than the C mice on Day 4 ($p < 0.05$). Furthermore, the RS mice showed a significantly longer latency on Day 5 ($p < 0.05$). These findings confirmed that the experimental conditions used in the present study were sufficiently stressful to impair the learning of mice. To test memory, the mice were re-subjected to the MWM test on Days 15 and 16 (Fig. 3). The C mice remembered the position of the platform well and shortened the escape latency for 2 days; whereas, the RS mice did not show an improved latency and had a significantly longer latency than the C mice ($p < 0.05$). On the other hand, the VE mice showed a shortened latency, which resulted in a significant difference between the RS and VE mice on Day 16 ($p < 0.05$). These findings suggest that voluntary exercise cures stress-induced impairment of cognitive function.

### 4.3. Neurogenesis in the SGZ of the dentate gyrus

To examine whether voluntary exercise restores hippocampal neurogenesis, we examined the number of Ki67- and BrdU-positive cells in the SGZ of the hippocampal dentate gyrus. In this study, we used Ki67-positive cells as a marker of the proliferation of new cells. On the other hand, since BrdU was injected 2 weeks before
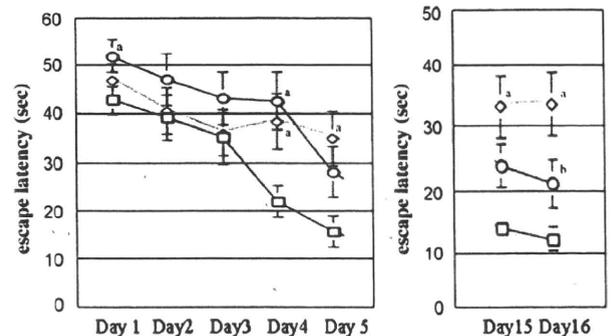


Fig. 3. Effects of voluntary exercise on escape latency as measured by Morris water maze test. RS mice showed significantly impaired escape latency of water maze test compared with C mice. The escape latency of VE mice was significantly shorter than RS mice. Significant difference of the escape latency between RS and VE mice was also observed on Days 15 and 16 of water maze test. The data is presented as the mean ± SE. [a] $p < 0.05$ vs. C mice. [b] $p < 0.05$ vs. RS mice.
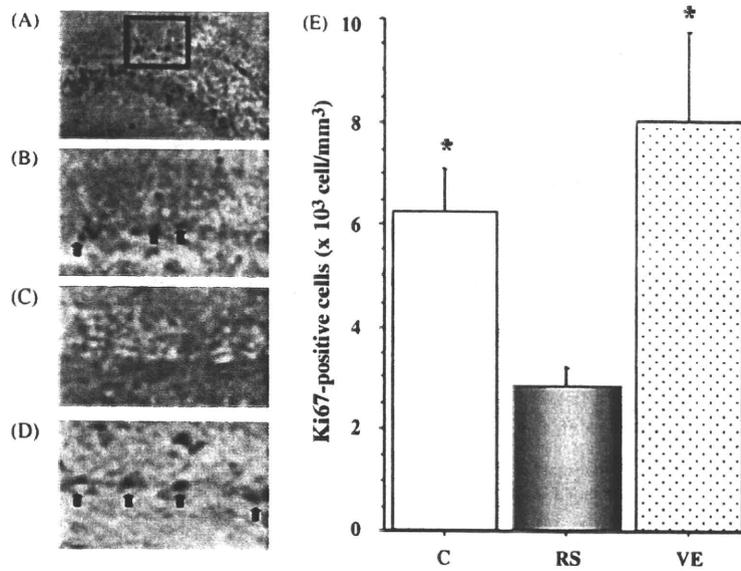
**Fig. 4.** Effects of voluntary exercise on the number of Ki67-positive cells in SGZ. (A) Representative photographs of Ki67-positive cells in SGZ are shown in Fig. 4A–D. (B) C mice, (C) RS mice, (D) VE mice. (E) The number of Ki67-positive cells in SGZ of dentate gyrus was significantly lower in RS mice than C and VE mice. There was no significant difference between C and VE mice. The data is shown as the mean ± SE. *$p < 0.05$ vs. RS mice.

dissection, we used BrdU-positive cells as a marker for the survival of new cells. The number of Ki67-positive cells in the SGZ of the dentate gyrus was significantly lower in the RS mice than in C or VE mice ($p < 0.05$) (Fig. 4). There was no significant difference between the C and VE mice. On the contrary, the number of BrdU-positive cells was significantly lower in the RS and VE mice compared with the C mice ($p < 0.05$) (Fig. 5). There was no significant difference between the RS and FE mice. These findings suggest that voluntary exercise attenuates stress-induced impairment of proliferation but does not improve the survival of new cells in the dentate gyrus.

### 4.4. 4-HNE positive cells in the GCL of the dentate gyrus

As shown in Fig. 6, the RS and VE mice had significantly more 4-HNE-positive cells in the GCL of the dentate gyrus than the C mice

($p < 0.05$). However, the VE mice had significantly fewer 4-HNE-positive cells compared with the RS mice ($p < 0.05$). These findings suggest that CRS increased lipid peroxidation in the dentate gyrus and that voluntary wheel running suppressed the accumulation of lipid peroxidation in stressed mice.

### 4.5. IGF-1 protein and mRNA

In this study, we focused on cerebral IGF-1 content because Carro et al. [24] reported that voluntary exercise enhances cell proliferation by increasing uptake of circulating IGF-1 into the brain. The VE mice showed a significant increase in the IGF-1 protein level in the cerebral cortex ($p < 0.05$). In addition, the VE mice showed a significantly higher level of IGF-1 mRNA in the liver than the C or RS mice ($p < 0.05$) (Fig. 7).
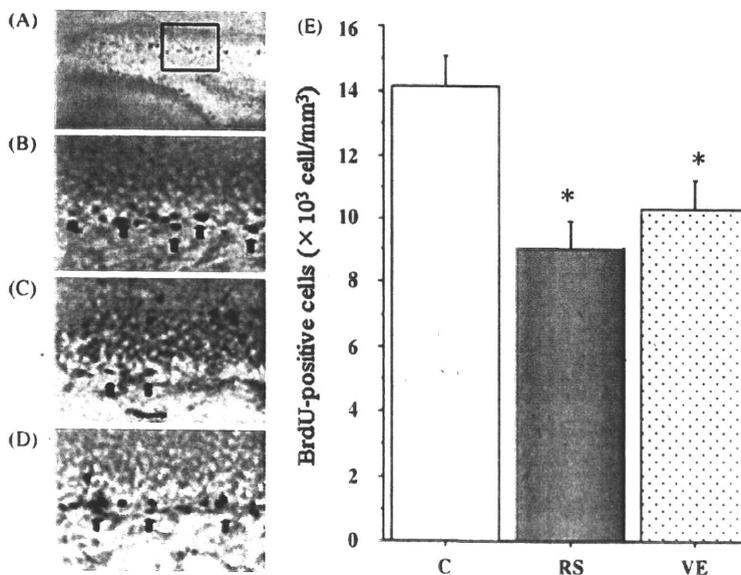


**Fig. 5.** Effects of voluntary exercise on the number of BrdU-positive cells in SGZ. (A) Representative photos of BrdU-positive-cells in SGZ are shown in Fig. 5A–D. (B) C mice, (C) RS mice, (D) VE mice. (E) Number of BrdU-positive cells in SGZ significantly lower in RS and VE mice than C mice. The data is shown as the mean ± SE. *$p < 0.05$ vs. C mice.
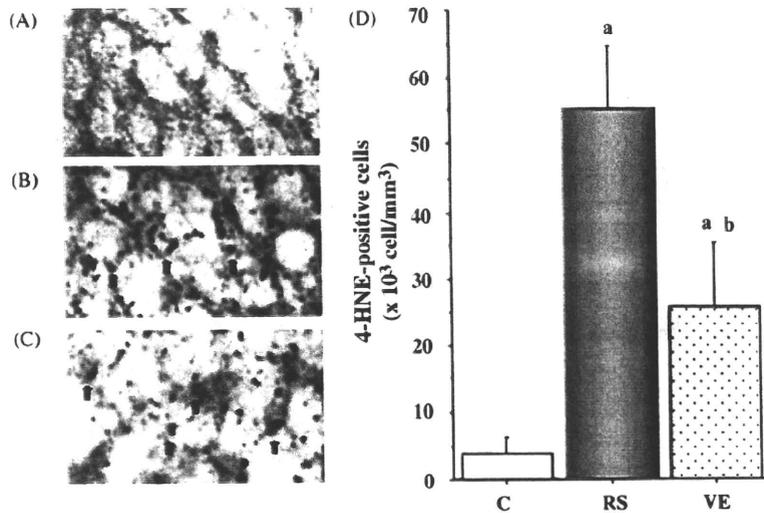
**Fig. 6.** Effects of voluntary exercise on the number of 4-HNE-positive cells in GCL. (A) Representative photos of 4-HNE-positive cells in GCL are shown in Fig. 6A–C. (A) C mice, (B) RS mice, (C) VE mice. (D) RS and VE mice had significantly more 4-HNE-positive cells in GCL of dentate gyrus than C mice. However, VE mice had significantly fewer 4-HNE-positive cells compared with RS mice. The data is shown as the mean ± SE. [a]$p < 0.05$ vs. C mice, [b]$p < 0.05$ vs. RS mice.

### 4.6. Antioxidant enzyme activity and α-tocopherol content

To examine the level of oxidative stress in the brains of the stressed mice, the α-tocopherol content of cerebral cortex was measured. The α-tocopherol content was significantly lower in the RS and VE mice than in the C mice ($p < 0.05$) (Fig. 8C).

To examine the antioxidant capacity of the stressed mice, SOD and GST activity in the brain were measured. There were no significant differences in hippocampal SOD activity between any groups of mice (Fig. 8A). However, GST activity was significantly higher in the VE mice than in the C or RS mice ($p < 0.05$) (Fig. 8B).

## 5. Discussion

To investigate whether voluntary exercise cures stress-induced impairment of cognitive function, the spatial memory of mice exposed to CRS with or without daily voluntary exercise was determined using the MWM test. Daily voluntary exercise attenuated the stress-induced impairment of cognitive function accompanied by improvement of the proliferation of new cells in the hippocampal

dentate gyrus and increases in the IGF-1 protein level in the cerebral cortex. In addition, daily voluntary exercise resulted in a decrease in the number of 4-HNE-positive cells in the GCL and increases in GST activity in the cerebral cortex. These findings suggest that habitual voluntary exercise prevents stress-induced impairment of cognitive function by retention of neurogenesis and inhibition of lipid peroxidation.

In this study, CRS, which involved daily immobilization for 12 h and feeding in a narrow cage, impaired cognitive function as evaluated by the MWM test (Fig. 3). This finding corresponds to the results of a previous study [5,8]. In addition, the present findings showed that voluntary exercise cures stress-induced impairment of cognitive function. This is the first report that has shown that voluntary exercise attenuate the stress-induced impairment of cognitive function.

Hippocampal neurogenesis is related to cognitive function. Nilsson et al. [29] reported that spatial memory is negatively correlated with hippocampal neurogenesis. We examined neurogenesis by dividing it into two phases, the proliferation and survival of newly born cells. Voluntary exercise restored the number of Ki67-positive cells but not BrdU-positive cells (Figs. 4 and 5), which suggested
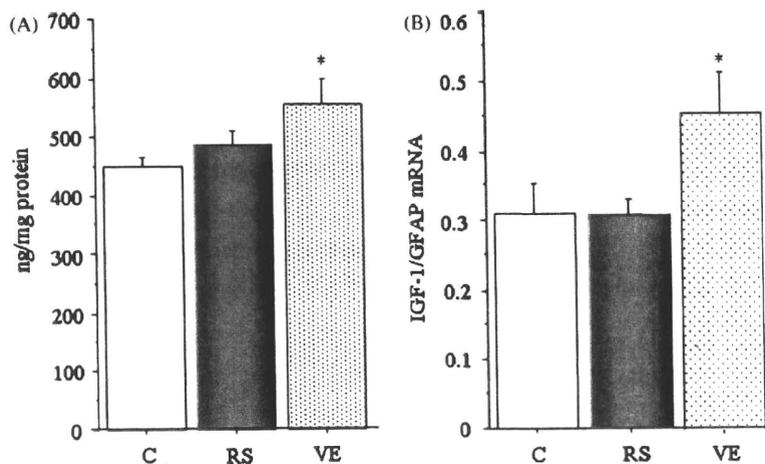


**Fig. 7.** Effects of voluntary exercise on IGF-1 in the cortex and IGF-1 mRNA in the liver. (A) VE mice showed significantly increased level of IGF-1 protein in the cortex than C and RS mice. The data is shown as the mean ± SE. (B) VE mice showed significantly increased level of IGF-1 mRNA in the liver than C and RS mice. The data is shown as the mean ± SE. *$p < 0.05$ vs. C and RS mice.
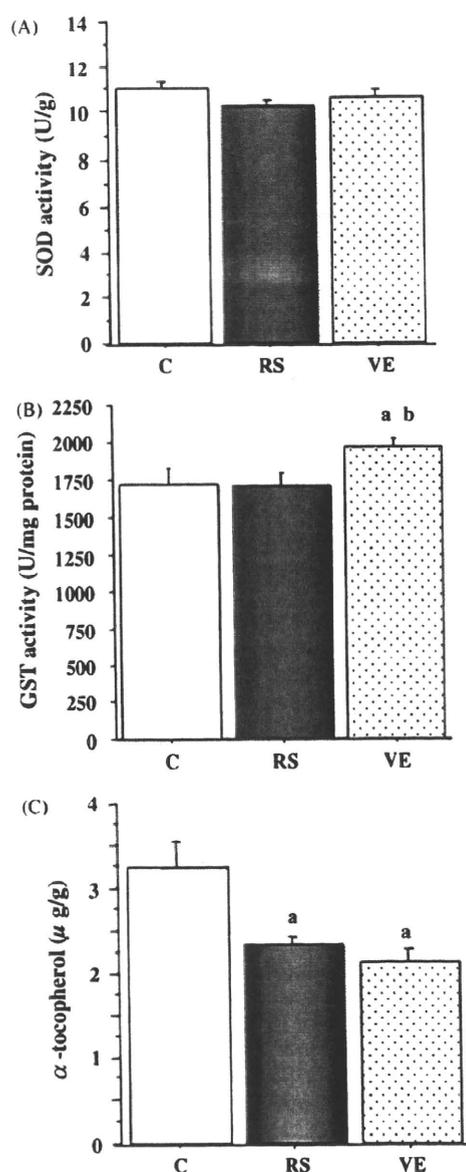
**Fig. 8.** Effects of voluntary exercise on SOD and GST activity and α-tocopherol content. (A). There was no significant difference in hippocampal SOD activity among three groups of the mice. (B) VE mice showed significantly increased levels of GST activity in the cortex than C and RS mice. (C) RS and VE mice had significantly decreased levels of α-tocopherol content in the cortex. The data is shown as the mean ± RS. $^a$$p < 0.05$ vs. C mice. $^b$$p < 0.05$ vs. RS mice.

the sedentary. Moreover, reported that IGF-1 produced in the liver is released into the cultural medium. Both IGF-1 mRNA and IGF-1 protein expression were significantly increased in the liver and cerebral cortex by voluntary exercise, respectively (Fig. 7A and B). These findings led us to expect that hepatic IGF-1 production was increased by voluntary exercise and that the IGF-1 produced in liver might be transported to the brain via the circulating blood, which led to an increase in IGF-1 protein in the cerebral cortex. IGF-1 injection leads to an increase of cell proliferation in the dentate gyrus of the hippocampus [33] Administration of anti-IGF-1 antibodies cancels out exercise-induced increases in cell proliferation in the dentate gyrus [25]. Combining the previous and present findings together supports the idea that voluntary exercise restores the proliferation of new cells by enhancing IGF-1 production in the liver and cerebral uptake of circulating IGF-1 derived from the liver.

Another interesting finding was the fact that voluntary exercise reduced the number of 4-HNE-positive cells in the SGZ (Fig. 6) without increasing SOD activity (Fig. 8A). SOD plays an important role in scavenging free radicals and preventing lipid peroxidation. Therefore, it was unexpected that the number of 4-HNE-positive cells would be reduced in VE mice without an increase in SOD activity. 4-HNE is a representative marker of lipid peroxidation [34]. The RS mice showed a significant increase in the number of 4-HNE-positive cells in the SGZ (Fig. 6), which supports the findings of our previous study [8]. In addition, the present findings showed decreases in α-tocopherol content in stressed mice (Fig. 8C), which supported the assertion that CRS leads to oxidative stress. The majority of cellular 4-HNE is metabolized via its conjugation to glutathione (GSH) through reactions catalyzed by GST [14,15]. The majority of GSH-HNE conjugate is transported into the extracellular environment through an ATP-dependent process catalyzed by Ral-interacting protein 76 (RLIP76) [35]. Ejchel-Cohen et al. [36] showed that 3 weeks of CRS downregulates GST mRNA expression in the hippocampus. In this study, the RS mice showed significant decreases in GST activity in the cerebral cortex compared with the C mice. In addition, the VE mice showed significant increases in GST activity compared with the C mice (Fig. 8B), which was in agreement with the previous finding that daily swimming exercise results in a significant increase in hepatic GST activity [13]. Therefore, the fact that voluntary exercise enhanced GST activity in the brain might have contributed to the significant reduction in the number of 4-HNE-positive cells in the SGZ. To clarify this, further investigation of the effects of GST expression on the level of protein and mRNA are necessary.

In conclusion, the present findings showed that voluntary exercise attenuated stress-induced impairment of cognitive function accompanied by improvement of cell proliferation in the dentate gyrus. This exercise-induced improvement is attributed to exercise-induced enhancement of IGF-1 protein and GST activity in the brain.

## Acknowledgement

## References

[1] Pawlak R, Rao BS, Melchor JP, Chattarji S, McEwen B, Strickland S. Tissue plasminogen activator and plasminogen mediate stress-induced decline of neuronal and cognitive functions in the mouse hippocampus. Proc Natl Acad Sci USA 2005;102:18201–6.
[2] Sousa N, Lukoyanov NV, Madeira MD, Almeida OF, Paula-Barbosa MM. Reorganization of the morphology of hippocampal neurites and synapses after stress-induced damage correlates with behavioral improvement. Neuroscience 2000;97:253–66.

that voluntary exercise was able to improve the proliferation of new cells in stressed mice but not survival. In normal mice, voluntary exercise enhances both the proliferation and survival of neuronal progenitor cells [30]. This contradiction may be attributed to differences in the experimental conditions or the normal or stressed mice. Chronic stress increases apoptotic cell death in hippocampal neurons [31,32]. Therefore, the reason why VE mice could not improve the cell survival of new cells might be because stress-induced increases in apoptotic cell death canceled out the effects of exercise on cell survival. However, we did not examine apoptosis cell in this study, so a further study is necessary to verify our speculation.

One of the factors that enhance cell proliferation in VE mice is an increase of IGF-1 in brain. Carro et al. [24] reported that physical exercise enhances the uptake of circulating IGF-1 compared

[3] Venero C, Tilling T, Hermans-Borgmeyer I, Schmidt R, Schachner M, Sandi C. Chronic stress induces opposite changes in the mRNA expression of the cell adhesion molecules NCAM and L1. Neuroscience 2002;115:1211–9.

[4] Jeong YH, Park CH, Yoo J, et al. Chronic stress accelerates learning and memory impairments and increases amyloid deposition in APPV717I-CT100 transgenic mice, an Alzheimer's disease model. FASEB J 2006;20:729–31.

[5] Nagata K, Nakashima-Kamimura N, Mikami T, Ohsawa I, Ohta S. Consumption of molecular hydrogen prevents the stress-induced impairments in hippocampus-dependent learning tasks during chronic physical restraint in mice. Neuropsychopharmacology 2009;34:501–8.

[6] Luo C, Xu H, Li XM. Quetiapine reverses the suppression of hippocampal neurogenesis caused by repeated restraint stress. Brain Res 2005;1063:32–9.

[7] Xu H, Chen Z, He J, et al. Synergetic effects of quetiapine and venlafaxine in preventing the chronic restraint stress-induced decrease in cell proliferation and BDNF expression in rat hippocampus. Hippocampus 2006;16:551–9.

[8] Nakajima S, Ohsawa I, Nagata K, et al. Oral supplementation with melon superoxide dismutase extract promotes antioxidant defences in the brain and prevents stress-induced impairment of spatial memory. Behav Brain Res 2009;200:15–21.

[9] Zafir A, Banu N. Antioxidant potential of fluoxetine in comparison to Curcuma longa in restraint-stressed rats. Eur J Pharmacol 2007;572:23–31.

[10] Akpinar D, Yargicoglu P, Derin N, Aslan M, Agar A. Effect of aminoguanidine on visual evoked potentials (VEPs), antioxidant status and lipid peroxidation in rats exposed to chronic restraint stress. Brain Res 2007;1186:87–94.

[11] Mikami T, Sumida S, Ishibashi Y, Ohta S. Endurance exercise training inhibits activity of plasma GOT and liver caspase-3 of mice [correction of rats] exposed to stress by induction of heat shock protein 70. J Appl Physiol 2004;96:1776–81.

[12] Kim JD, Yu BP, McCarter RJ, Lee SY, Herlihy JT. Exercise and diet modulate cardiac lipid peroxidation and antioxidant defenses. Free Radic Biol Med 1996;20:83–8.

[13] Reddy KV, Anuradha D, Kumar TC, Reddanna P. Induction of Ya1 subunit of rat hepatic glutathione S-transferases by exercise-induced oxidative stress. Arch Biochem Biophys 1995;323:6–10.

[14] Hartley DP, Ruth JA, Petersen DR. The hepatocellular metabolism of 4-hydroxynonenal by alcohol dehydrogenase, aldehyde dehydrogenase, and glutathione S-transferase. Arch Biochem Biophys 1995;316:197–205.

[15] Srivastava SK, Hu X, Xia H, et al. ATP-dependent transport of glutathione conjugate of 7beta, 8alpha-dihydroxy-9alpha,10alpha-oxy-7,8,9,10-tetrahydrobenzo[a]pyrene in murine hepatic canalicular plasma membrane vesicles. Biochem J 1998;332(Pt 3):799–805.

[16] Ding Q, Vaynman S, Akhavan M, Ying Z, Gomez-Pinilla F. Insulin-like growth factor I interfaces with brain-derived neurotrophic factor-mediated synaptic plasticity to modulate aspects of exercise-induced cognitive function. Neuroscience 2006;140:823–33.

[17] van Praag H, Christie BR, Sejnowski TJ, Gage FH. Running enhances neurogenesis, learning, and long-term potentiation in mice. Proc Natl Acad Sci USA 1999;96:13427–31.

[18] van Praag H, Kempermann G, Gage FH. Running increases cell proliferation and neurogenesis in the adult mouse dentate gyrus. Nat Neurosci 1999;2:266–70.

[19] Farmer J, Zhao X, van Praag H, Wodtke K, Gage FH, Christie BR. Effects of voluntary exercise on synaptic plasticity and gene expression in the dentate gyrus of adult male Sprague–Dawley rats in vivo. Neuroscience 2004;124:71–9.

[20] van Praag H, Shubert T, Zhao C, Gage FH. Exercise enhances learning and hippocampal neurogenesis in aged mice. J Neurosci 2005;25:8680–5.

[21] Mirochnic S, Wolf S, Staufenbiel M, Kempermann G. Age effects on the regulation of adult hippocampal neurogenesis by physical activity and environmental enrichment in the APP23 mouse model of Alzheimer disease. Hippocampus 2009.

[22] Wolf SA, Kronenberg G, Lehmann K, et al. Cognitive and physical activity differently modulate disease progression in the amyloid precursor protein (APP)-23 model of Alzheimer's disease. Biol Psychiatry 2006;60:1314–23.

[23] Mattson MP, Duan W, Wan R, Guo Z. Prophylactic activation of neuroprotective stress response pathways by dietary and behavioral manipulations. NeuroRx 2004;1:111–6.

[24] Carro E, Nunez A, Busiguina S, Torres-Aleman I. Circulating insulin-like growth factor I mediates effects of exercise on the brain. J Neurosci 2000;20:2926–33.

[25] Carro E, Trejo JL, Busiguina S, Torres-Aleman I. Circulating insulin-like growth factor I mediates the protective effects of physical exercise against brain insults of different etiology and anatomy. J Neurosci 2001;21:5678–84.

[26] Morris R. Developments of a water-maze procedure for studying spatial learning in the rat. J Neurosci Methods 1984;11:47–60.

[27] Habig WH, Pabst MJ, Jakoby WB. Glutathione S-transferases. The first enzymatic step in mercapturic acid formation. J Biol Chem 1974;249:7130–9.

[28] Milne DB, Botnen J. Retinol. alpha-tocopherol, lycopene, and alpha- and beta-carotene simultaneously determined in plasma by isocratic liquid chromatography. Clin Chem 1986;32:874–6.

[29] Nilsson M, Perfilieva E, Johansson U, Orwar O, Eriksson PS. Enriched environment increases neurogenesis in the adult rat dentate gyrus and improves spatial memory. J Neurobiol 1999;39:569–78.

[30] Trejo JL, Carro E, Torres-Aleman I. Circulating insulin-like growth factor I mediates exercise-induced increases in the number of new neurons in the adult hippocampus. J Neurosci 2001;21:1628–34.

[31] Zhu X, Cheng M, Peng M, Xiao X, Yao S, Zhang X. Basal behavioral characterization of hsf1 deficient mice and its cellular and behavioral abnormalities underlying chronic unpredictable stressors. Behav Brain Res 2008;193:225–9.

[32] Tobe I, Ishida Y, Tanaka M, Endoh H, Fujioka T, Nakamura S. Effects of repeated maternal stress on FOS expression in the hypothalamic paraventricular nucleus of fetal rats. Neuroscience 2005;134:387–95.

[33] Carro E, Torres-Aleman I. Serum insulin-like growth factor I in brain function. Keio J Med 2006;55:59–63.

[34] Esterbauer H, Schaur RJ, Zollner H. Chemistry and biochemistry of 4-hydroxynonenal, malonaldehyde and related aldehydes. Free Radic Biol Med 1991;11:81–128.

[35] Awasthi S, Cheng J, Singhal SS, et al. Novel function of human RLIP76: ATP-dependent transport of glutathione conjugates and doxorubicin. Biochemistry 2000;39:9327–34.

[36] Ejchel-Cohen TF, Wood GE, Wang JF, et al. Chronic restraint stress decreases the expression of glutathione S-transferase pi2 in the mouse hippocampus. Brain Res 2006;1090:156–62.

# Preventive effects of *Chlorella* on cognitive decline in age-dependent dementia model mice

Yuya Nakashima [a], Ikuroh Ohsawa [b,c], Fumiko Konishi [a], Takashi Hasegawa [a], Shoichiro Kumamoto [a], Yoshihiko Suzuki [b], Shigeo Ohta [b,*]

[a] Research Laboratories, Chlorella Industry Co. Ltd., 1343 Hisatomi, Chikugo, Fukuoka 833-0056, Japan
[b] Department of Biochemistry and Cell Biology, Institute of Development and Aging Sciences, Nippon Medical School,
1-396 Kosugi-cho, Nakahara-ku, Kawasaki, Kanagawa 211-8533, Japan
[c] The Center of Molecular Hydrogen Medicine, Institute of Development and Aging Sciences, Nippon Medical School, Kawasaki, Kanagawa 211-8533, Japan

## ARTICLE INFO

## ABSTRACT

Oxidative stress is one of the major causes of age-dependent memory loss and cognitive decline. Cytotoxic aldehydes are derived from lipid peroxides and their accumulation may be responsible for age-dependent neurodegeneration, including Alzheimer's disease. Since aldehyde dehydrogenases detoxify such aldehydes, we constructed transgenic mice with mitochondrial aldehyde dehydrogenase 2 (ALDH2) activity deficiency (DAL101 mice) as an age-dependent dementia model. This model animal is age-dependently progressed by persistent oxidative stress, and thus enables us to investigate foods that prevent dementia. Since *Chlorella*, a kind of alga, exhibits various anti-oxidative effects, we investigated whether *Chlorella* has the potential to prevent age-dependent cognitive impairment. We fed *Chlorella* to DAL101 mice and investigated its effects on oxidative stress and the progression of cognitive decline using the Morris water-maze and object recognition tests. The diet with *Chlorella* tended to reduce oxidative stress and significantly prevented the decline of cognitive ability, as shown by both methods. Moreover, consumption of *Chlorella* decreased the number of activated astrocytes in the DAL101 brain. These findings suggest that the prolonged consumption of *Chlorella* has the potential to prevent the progression of cognitive impairment.

© 2009 Elsevier Ireland Ltd. All rights reserved.

The decline of cognitive ability in Alzheimer's disease (AD) is associated with aging, and may be caused by persistent oxidative stress in the brain [13]. Highly reactive aldehydes, such as 4-hydroxy-2-nonenal (4-HNE), are spontaneously generated from lipid peroxides [24]. In particular, 4-HNE rapidly reacts with most biomolecules and injures living cells [29]. In fact, increased levels of 4-HNE-modified proteins in the brain of AD and Parkinson disease (PD) patients have been observed [11,33]. These findings imply that antioxidants that can reduce oxidative stress play important roles in the prevention of cognitive impairment and neurodegeneration; however, most clinical trials supplying a single dietary antioxidant have not resulted in great success in preventing dementia [12,19,23].

Dominant-negative-type aldehyde dehydrogenase 2 (ALDH2) is present in Mongoloids. Japanese, Korean and Chinese groups have independently reported that the genetic polymorphism (ALDH2*2) is a risk for AD [4,5,30]. Cells expressing ALDH2*2 are vulnerable to 4-HNE, and cell death is induced by treatment with 4-HNE [15,18].

To investigate the role of such toxic aldehydes, we constructed transgenic mice expressing a dominant-negative form of ALDH2 (ALDH2*2) in the brain (DAL101 mice) [16]. The mice had decreased ability to detoxify 4-HNE in their cortical neurons and accelerated accumulation of 4-HNE in the brain. Consequently, their lifespan was shortened and age-dependent neurodegeneration and hyperphosphorylation of tau were observed. The onset of cognitive impairment correlated with neurodegeneration, which was further accelerated by APOE knockout. No obvious pathological features, including cognitive function, were observed in young DAL101 mice, indicating that no physiological and neurological changes would occur during their aging. After maturation, oxidative stress accumulated in the brain and cognitive deficits developed in aged DAL101 [16,17]. The importance of this model mouse is the age-dependent onset of neurodegenerative disorders. Thus, this model animal will be helpful to explore foods that can prevent age-dependent dementia.

*Chlorella* is a kind of alga. It and its extract with hot water have long been used as health foods. It was reported that *Chlorella* exhibits various immunopharmacological effects [1,6,28] and functions as an antioxidant *in vitro* and *in vivo* [10,22,26], probably

* Corresponding author. Tel.: +81 44 733 9267; fax: +81 44 733 9268.
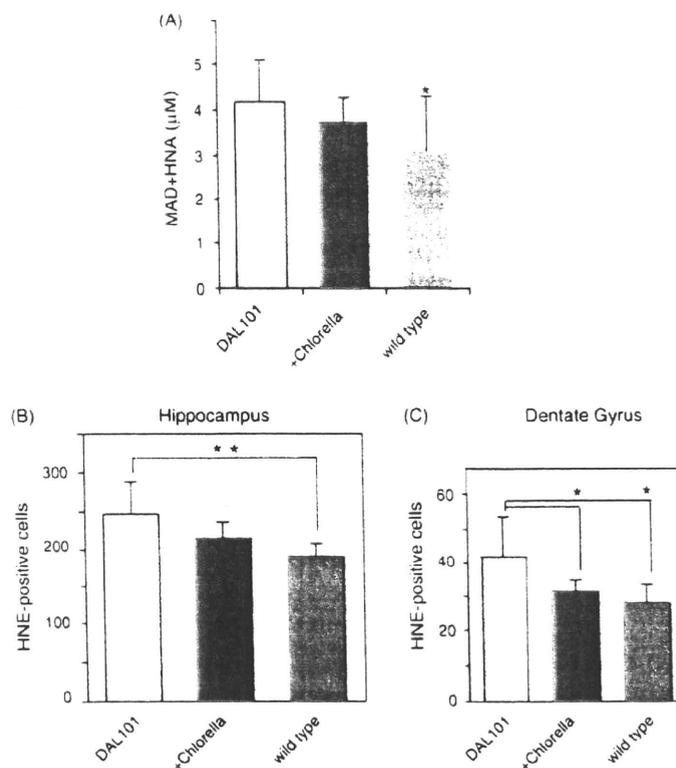   *E-mail address:* ohta@nms.ac.jp (S. Ohta).

355

Fig. 1. Effects of *Chlorella* consumption on oxidative stress. (A) Total blood MDA + HNA was measured after 16-month *Chlorella* administration. (B and C) HNE-positive cells were counted in the whole hippocampus (B) and the datate gyrus region (C). DAL101: DAL101 normal diet ($n = 10$), +Chlorella: DAL101 with *Chlorella* diet ($n = 6$), and wild type: C57BL/6 with normal diet ($n = 8$). *$p < 0.05$: significant DAL101 vs. wild type.

because it is rich in chlorophyll and carotenoids, including β-carotene and lutein.

In this study, we fed *Chlorella* to age-dependent dementia model mice for a prolonged period, and suggest that *Chlorella* has potential for preventing age-dependent dementia.

We constructed transgenic mice, expressing a dominant-negative form of ALDH2 (ALDH2*2) in the brain (DAL101 mice) as previously reported [16]. DAL101 mice were fed the basic diet CE-2 (Clea Japan, Tokyo) (control group) or a 5% *Chlorella*-supplemented diet (*Chlorella* treatment group) for 16 months from 8 weeks of age.

The wild-type mice, C57BL/6 (Kyudo, Fukuoka, Japan), were also fed the basic diet CE-2 as a normal group. The animals were given free access to water and food. The body weight was measured weekly.

*Chlorella* used for the diet preparation was the *Parachlorella beyerinckii* CK-5 strain, cultured, dried, and powdered by Chlorella Industry Co., Ltd. Animals were maintained following the Animal Experiment Guideline of Chlorella Industry Co., Ltd., established in accordance with the 'Standards Concerning Maintenance and Storage of Experimental Animals' (Notice No. 6 from the Prime Minister's Office on March 27, 1980, partially revised on May 28, 2002).

Mice were trained on the Morris water-maze [14,16]. The water-maze was a circular pool filled with opaque water at room temperature (diameter, 1.1 m). A transparent platform (diameter, 10 cm) was hidden 1 cm below the surface. If a mouse failed to find the platform within 60 s, it was guided carefully to the platform and allowed to remain there for 20 s. Mice were given four trials a day for 5 days. The examiner determined the time of swimming until

the mouse reached the platform (latency). Retention of the spatial training was assessed 24 h after the last training trial. A single probe trial consisted of a 60 s free swim in the pool without the platform.

The visual object recognition test (vORT) was used to test recognition memory [16,31]. Mice were first habituated in a cage for 24 h before training. During 10 min of training, two plastic blocks with different shapes and colors were presented. Object recognition was scored by the number of approaches to and/or sniffs of the object and shown as percentage preference (recognition index). One day after training, one of the conditioned blocks was replaced with a novel object to test for memory retention, and recognition index was scored during 5 min of testing.

For immunohistochemistry, the brain was fixed for 24 h by using 4% paraformaldehyde in PBS and embedded in paraffin. Tissues were sectioned and immunostained with an oxidative stress marker, anti-HNE antibody (Kikken Seil Co., Fukuroi, Japan), a gliosis marker anti-Iba-1 antibody (COVANCE) and an astrocyte marker anti-glial fibrillary acidic protein (GFAP) antibody (clone GA5; Millipore). As an alternative oxidative stress marker, blood malondialdehyde (MDA) and hydroxyalkenale (HNA) levels were determined using a Bioxytech MDA-586 Assay Kit (OxisResearch, Oregon, USA) according to the instruction manual.

For statistical analysis, all values were shown as the mean ± the standard deviation (SD). One-way ANOVA (Fisher's PLSD test) followed by contrast testing was used to compare the data from multiple groups. Statistical significance was accepted as $p < 0.05$. We performed quantification experiments in a blinded fashion.

To investigate the effects of 16-month *Chlorella* consumption in DAL101 mice, we measured total amounts of MDA and HNA in
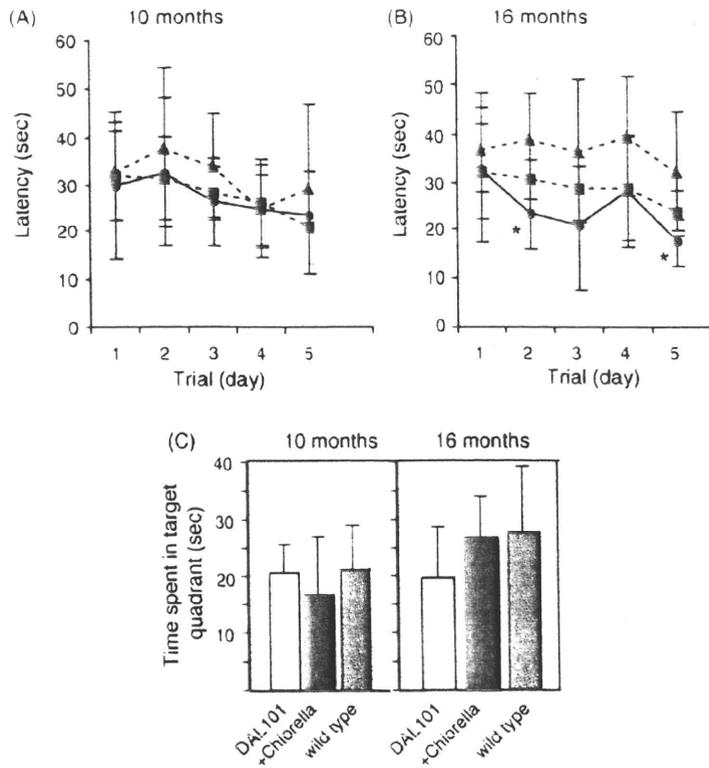
**Fig. 2.** Effects of *Chlorella* consumption on spatial memory and learning ability. The Morris water-maze test was performed after 10-month (A) and 16-month (B) *Chlorella* consumption. Four trials per day were repeated for 5 days, and the time required to reach the platform (latency time) was measured. When the animal could not reach the platform within 60 s, the latency time was regarded as 60 s. Closed triangle: DAL101 normal diet (n = 5), closed circle: DAL101 with *Chlorella* diet (n = 5), and closed square: C57BL/6 with normal diet (n = 5). (C) Probe trials after 10- and 16-month *Chlorella* consumption. The platform was removed the day after completing the 5-day training trial, and a 60-second probe trial was performed. The time spent in the quadrant in which the platform was previously present was shown as % to wild type. DAL101: DAL101 normal diet (n = 5), +Chlorella: DAL101 with *Chlorella* diet (n = 5), and wild type: C57BL/6 with normal diet (n = 5). *p < 0.05: significant vs. DAL101 (normal diet).

blood as well as HNE-positive cells in the brain as oxidative stress markers. MDA and HNA level in blood and HNE-positive cells in the hippocampus were significantly higher in DAL101 than in wild-type C57BL/6 mice, whereas the *Chlorella* diet did not significantly improve the oxidative stress level (Fig. 1A and B). However, the number of HNE-positive cells was reduced by the *Chlorella* diet in the dentate gyrus region of hippocampus (Fig. 1C), suggesting that the *Chlorella* diet seems to improve oxidative stress.

The body weight of DAL101 mice (male and female) tended to be lighter than wild-type C57BL/6 mice, suggesting that ALDH2
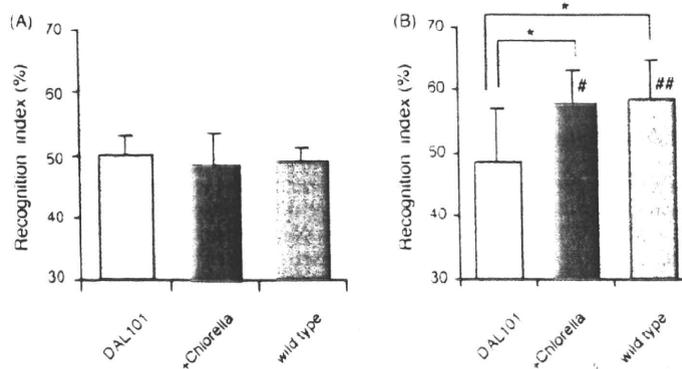


**Fig. 3.** Effects of *Chlorella* consumption on recognition and learning ability. (A) Training for the object recognition test was performed after 16-month *Chlorella* consumption. The frequencies of exploratory behavior towards 2 objects were measured, and the percent ratios of the frequencies were calculated (recognition index). (B) The frequencies of exploratory behavior towards the 2 objects were measured on the day following the training trial, and the percent ratio of the frequency of exploratory behavior toward the novel object was calculated. DAL101: DAL101 normal diet (n = 8), +Chlorella: DAL101 with *Chlorella* diet (n = 5), and wild type: C57BL/6 with normal diet (n = 6). *p < 0.05: significant vs. DAL101 (normal diet). #p < 0.05, ##p < 0.01: significant vs. training trial.